

**Fig. 3** Susceptibility of melanoma cell lines to mHag-specific CTL clones and the impact of cytokine treatment. **a** <sup>51</sup>Cr-release assay against melanoma cell lines. Standard 4-h <sup>51</sup>Cr-release assays were performed against various melanoma cell lines at the indicated E/T ratios and at least in duplicate. B-LCLs positive for the restriction HLA allele and mHag allele were used as positive controls for individual CTL clones. The 721.221 cell line comprised HLA-A\*0201-transduced B-LCLs positive for the HA-1<sup>H</sup> allele. Non-

specific lysis of the individual CTL clones was examined and verified by testing against NK cell-sensitive K562 or melanoma cell lines that lacked either the cognate mHag or restriction HLA allele. I/T denotes the treatment of indicated cell lines with 500 U/mL of IFN-γ and 10 ng/mL of TNF-α for 48 hours prior to assays; **b** HLA class I and BCL2A1 expression of melanoma cell lines. Cell surface expression of HLA class I and intracellular staining of BCL2A1 was evaluated by flow cytometry before and after treatment with the above cytokines

### 3.4 HMHA1 in dermal fibroblasts is also upregulated by inflammatory cytokines

It has been reported that *HMHA1* encoding HA-1 mHag is not detected in normal nonhematopoietic cells such as dermal fibroblasts [9], while *BCL2A1* is upregulated in bone marrow-derived mesenchymal stem cells by inflammatory cytokines [16]. Thus, we examined whether dermal fibroblasts upregulated these mHag genes and became susceptible to cognate CTL clones. We found that the expression of both *BCL2A1* and *HMHA1* is upregulated in the dermal fibroblasts after cytokine treatment (Fig. 1a, b, upper part), indicating that these hematopoietic cell-specific mHags might be induced in a strong inflammatory cytokine milieu such as active GVHD after HSCT. Hematopoietic cell contamination was excluded by real-time PCR or flow cytometric analysis of the expression of CD45 in these fibroblasts (data not shown). Coincident with expression, the HLA-A\*0201-restricted HA-1<sup>H</sup>-specific CTL clone, EH6-CTL, and A\*2402 restricted ACC-1<sup>Y</sup> specific CTL clone, 18B3-CTL, could lyse these cytokine-treated mHag-positive dermal fibroblasts, although their

level of lysis was relatively lower than that of hematopoietic cells (Fig. 4a, b).

## 4 Discussion

In this study, we demonstrated that HLA-A24-restricted ACC-1<sup>Y</sup> and HLA-B44-restricted ACC-2<sup>D</sup> mHags, whose expressions were shown to be limited to hematopoietic cells including leukemia cells, were also expressed in melanoma cell lines by real-time PCR and cytotoxicity assays. Melanoma is known as one of the representative immunogenic tumors. Previously, IL-2 administration [4] or the infusion of ex vivo expanded TILs [17] was tested, but resulted in a limited clinical response. In 1990s, many antigens of melanoma origin recognized by autologous T lymphocytes were identified [18], and these antigens were subsequently tested in clinical trials by peptide vaccination or adoptive CTL infusion. To date, peptide vaccination has resulted in a limited or marginal efficacy [19] while adoptive T lymphocyte infusion including Ag-specific CTL clones or TILs, especially after a lymphodepleted conditioning regimen,

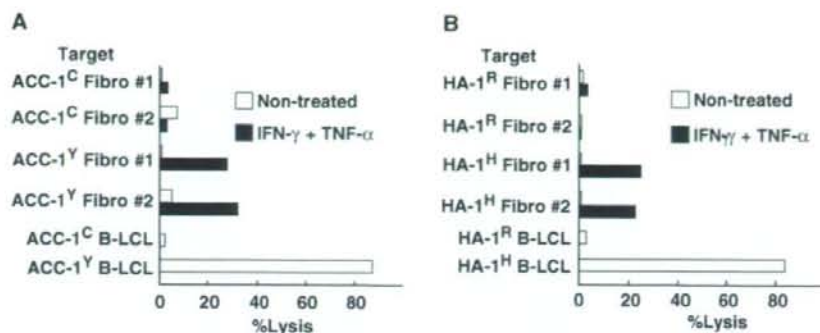


**Fig. 4** Cytotoxicity of mHag-specific CTL clones against dermal fibroblasts. A standard 4-h  $^{51}\text{Cr}$ -release assay was performed, as described above. **a** Cytotoxic activity of the HLA-A\*2402-restricted, ACC-1<sup>Y</sup> mHag-specific 1B3-CTL clone against HLA-A\*2402-positive dermal fibroblasts (Fibro) and B-LCLs that were either ACC-1<sup>Y</sup> mHag allele positive or negative (indicated as ACC-1<sup>C</sup>);

**b** cytotoxic activity of the HLA-A\*0201-restricted, HA-1<sup>H</sup>-specific EH6-CTL clone against HLA-A\*0201-positive dermal fibroblasts and B-LCLs that were either HA-1<sup>H</sup> mHag allele positive or negative (indicated as HA-1<sup>R</sup>). IFN- $\gamma$  + TNF- $\alpha$  treatment was performed as described in Fig. 3. The effector target ratio was fixed at 30:1

demonstrated promising results [20–22]. After allogeneic HSCT for patients with melanoma, there have been some reports indicating that CTLs against melanoma cells do exist and that these melanoma-reactive CTLs can be expanded in vitro [23, 24]. These observations suggest that allogeneic HSCT after a nonmyeloablative conditioning regimen might be a promising therapeutic strategy for patients with refractory metastatic melanoma.

Childs et al., however, reported relatively disappointing results in which 5 out of 11 metastatic melanoma patients receiving allogeneic HSCT died from rapid tumor growth, while the rest of the patients showed variable results [14]. As in the case of hematological malignancies, a high tumor burden should be one of the most unfavorable factors regarding treatment failure with allogeneic HSCT. Therefore, a treatment strategy combining the selection of patients with a lower tumor burden or slower growth kinetics and allogeneic HSCT may be explored for this poor-prognosis disease if the given donor and recipient are eligible for immunotherapy using ACC-1 and ACC-2 mHags, or other hematopoiesis-specific mHags are also highly expressed in melanoma cells. Since HSCT recipients eligible for ACC-1, ACC-2, and HA-1 mHags exist at a frequency of 11, 3, and 9%, respectively, in Japanese [25], it would be possible to apply these mHags to nearly a quarter of such patients.

BCL2A1 is a member of the B-cell lymphoma-2 (BCL2) family. BCL2 is highly expressed in melanoma, which was shown to contribute to a chemoresistant phenotype [26]. The reduction of BCL2 by siRNA caused melanoma cells to become susceptible to chemotherapeutic agents. BCL2A1, although regulated differently from BCL2, also exerts antiapoptotic activity and is expressed even in normal melanocytes like other melanocyte differentiating

antigens, such as Melan-A/MART-1 or tyrosinase. In this regard, BCL2A1 would be essential for melanoma cells and melanocyte survival, suggesting that it may be a good candidate antigen for immunotherapy against melanoma, although autoimmune depigmentation may also develop, as seen in adoptive immunotherapy targeting melanoma-associated antigens mentioned above [20, 21].

In addition, we unexpectedly found that, after cytokine treatment, dermal fibroblasts upregulated both *BCL2A1* and *HMHA1* expression and become susceptible to cognate CTL clones, respectively (Fig. 4). This suggests that, after allogeneic HSCT, they would also be upregulated under a “cytokine-storm”, and may contribute in some way to the pathophysiology of skin GVHD. In the clinical setting, HA-1 was originally reported as an mHag associated with GVHD [27], and additional studies brought about mixed results, making it still too early to draw any conclusion [28, 29], while ACC-1<sup>Y</sup> disparity did not seem to be associated with an increased incidence of acute GVHD [30]. In skin explant assays, it was shown that skin sections from HLA-A2\* HA-1\* individuals incubated with HA-1 CTLs developed only background grade I or low grade II GVH reactions, while male HLA-A2\* skin sections incubated with Y antigen-specific CTLs displayed severe GVH reactions of grade III–IV [31]. It is assumed that stronger GVH reactions might be observed if skin sections are pretreated with cytokines before incubation with HA-1-specific CTLs. IFN- $\gamma$ , which is known to induce various transcription factors specific for hematopoiesis and immunity, might be a key in this upregulation of hematopoietic cell-restricted mHags in dermal fibroblasts. Since IFN- $\gamma$  is strongly produced by CTLs and type 1 helper T cells, the IFN- $\gamma$  secreted from mHag-specific CTLs could lead to the upregulation of target hematopoiesis-specific

mHags, resulting in GVHD or GVT effects in tumors sensitive to the IFN- $\gamma$ -induced upregulation of such mHags. Therefore, it is crucial to develop a new treatment strategy to induce selective GVT effects while avoiding life-threatening GVHD using preconditioning and GVHD prophylaxis regimens to minimize GVHD, followed by selective immunotherapy targeting mHags mainly expressed in tumors and hematopoietic cells, such as ACC-1, -2, and HA-1, after the "cytokine storm" period is over.

In summary, *BCL2A1*-encoded mHags, ACC-1 and ACC-2, may be potential targets of immunological interventions for a fraction of patients with refractory, but not bulky melanoma following allogeneic HSCT.

## References

- den Haan JM, Meadows LM, Wang W, et al. The minor histocompatibility antigen HA-1: a diallelic gene with a single amino acid polymorphism. *Science*. 1998;279:1054–7.
- Kawase T, Akatsuka Y, Torikai H, et al. Alternative splicing due to an intronic SNP in HMSD generates a novel minor histocompatibility antigen. *Blood*. 2007;110:1055–63.
- Bleakley M, Riddell SR. Molecules and mechanisms of the graft-versus-leukaemia effect. *Nat Rev Cancer*. 2004;4:371–80.
- Atkins MB, Lotze MT, Dutcher JP, et al. High-dose recombinant interleukin 2 therapy for patients with metastatic melanoma: analysis of 270 patients treated between 1985 and 1993. *J Clin Oncol*. 1999;17:2105–16.
- McDermott DF. Update on the application of interleukin-2 in the treatment of renal cell carcinoma. *Clin Cancer Res*. 2007;13:716s–20s.
- Ravaud A, Dilhuydy MS. Interferon alpha for the treatment of advanced renal cancer. *Expert Opin Biol Ther*. 2005;5:749–62.
- Bishop MR, Fowler DH, Marchigiani D, et al. Allogeneic lymphocytes induce tumor regression of advanced metastatic breast cancer. *J Clin Oncol*. 2004;22:3886–92.
- Childs R, Chernoff A, Contentin N, et al. Regression of metastatic renal-cell carcinoma after nonmyeloablative allogeneic peripheral-blood stem-cell transplantation. *N Engl J Med*. 2000;343:750–8.
- Klein CA, Wilke M, Pool J, et al. The hematopoietic system-specific minor histocompatibility antigen HA-1 shows aberrant expression in epithelial cancer cells. *J Exp Med*. 2002;196:359–68.
- Fujii N, Hiraki A, Ikeda K, et al. Expression of minor histocompatibility antigen, HA-1, in solid tumor cells. *Transplantation*. 2002;73:1137–41.
- Miyazaki M, Akatsuka Y, Nishida T, et al. Potential limitations in using minor histocompatibility antigen-specific cytotoxic T cells for targeting solid tumor cells. *Clin Immunol*. 2003;107:198–201.
- Slager EH, Honders MW, van der Meijden ED, et al. Identification of the angiogenic endothelial-cell growth factor-1/thymidine phosphorylase as a potential target for immunotherapy of cancer. *Blood*. 2006;107:4954–60.
- Akatsuka Y, Nishida T, Kondo E, et al. Identification of a polymorphic gene, *BCL2A1*, encoding two novel hematopoietic lineage-specific minor histocompatibility antigens. *J Exp Med*. 2003;197:1489–500.
- Childs R, Srinivasan R. Advances in allogeneic stem cell transplantation: directing graft-versus-leukemia at solid tumors. *Cancer J*. 2002;8:2–11.
- Su AI, Cooke MP, Ching KA, et al. Large-scale analysis of the human and mouse transcriptomes. *Proc Natl Acad Sci USA*. 2002;99:4465–70.
- Kloosterboer FM, van Luxemburg-Heijs SA, van Soest RA, van Egmond HM, Willemze R, Falkenburg JH. Up-regulated expression in nonhematopoietic tissues of the *BCL2A1*-derived minor histocompatibility antigens in response to inflammatory cytokines: relevance for allogeneic immunotherapy of leukemia. *Blood*. 2005;106:3955–7.
- Khammari A, Nguyen JM, Pandolfino MC, et al. Long-term follow-up of patients treated by adoptive transfer of melanoma tumor-infiltrating lymphocytes as adjuvant therapy for stage III melanoma. *Cancer Immunol Immunother*. 2007;56:1853–60.
- Boon T, Coulic PG, Van den Eynde BJ, van der Bruggen P. Human T cell responses against melanoma. *Annu Rev Immunol*. 2006;24:175–208.
- Machiels JP, van Baren N, Marchand M. Peptide-based cancer vaccines. *Semin Oncol*. 2002;29:494–502.
- Yee C, Thompson JA, Byrd D, et al. Adoptive T cell therapy using antigen-specific CD8+ T cell clones for the treatment of patients with metastatic melanoma: in vivo persistence, migration, and antitumor effect of transferred T cells. *Proc Natl Acad Sci USA*. 2002;99:16168–73.
- Dudley ME, Wunderlich JR, Robbins PF, et al. Cancer regression and autoimmunity in patients after clonal repopulation with antitumor lymphocytes. *Science*. 2002;298:850–4.
- Dudley ME, Wunderlich JR, Yang JC, et al. Adoptive cell transfer therapy following non-myeloablative but lymphodepleting chemotherapy for the treatment of patients with refractory metastatic melanoma. *J Clin Oncol*. 2005;23:2346–57.
- Kurokawa T, Fischer K, Bertz H, Hoegerle S, Finke J, Mackensen A. In vitro and in vivo characterization of graft-versus-tumor responses in melanoma patients after allogeneic peripheral blood stem cell transplantation. *Int J Cancer*. 2002;101:52–60.
- Gottlieb DJ, Li YC, Lionello I, et al. Generation of tumour-specific cytotoxic T-cell clones from histocompatibility leucocyte antigen-identical siblings of patients with melanoma. *Br J Cancer*. 2006;95:181–8.
- Akatsuka Y, Morishima Y, Kuzushima K, Kodera Y, Takahashi T. Minor histocompatibility antigens as targets for immunotherapy using allogeneic immune reactions. *Cancer Sci*. 2007;98:1139–46.
- Vlaykova T, Talve L, Hakka-Kemppinen M, et al. Immunohistochemically detectable bcl-2 expression in metastatic melanoma: association with survival and treatment response. *Oncology*. 2002;62:259–68.
- Goulmy E, Schipper R, Pool J, et al. Mismatches of minor histocompatibility antigens between HLA-identical donors and recipients and the development of graft-versus-host disease after bone marrow transplantation. *N Engl J Med*. 1996;334:281–5.
- Tseng LH, Lin MT, Hansen JA, et al. Correlation between disparity for the minor histocompatibility antigen HA-1 and the development of acute graft-versus-host disease after allogeneic marrow transplantation. *Blood*. 1999;94:2911–4.
- Murata M, Emi N, Hirabayashi N, et al. No significant association between HA-1 incompatibility and incidence of acute graft-versus-host disease after HLA-identical sibling bone marrow transplantation in Japanese patients. *Int J Hematol*. 2000;72:371–5.
- Nishida T, Akatsuka Y, Morishima Y, et al. Clinical relevance of a newly identified HLA-A24-restricted minor histocompatibility antigen epitope derived from *BCL2A1*. ACC-1, in patients receiving HLA genotypically matched unrelated bone marrow transplant. *Br J Haematol*. 2004;124:629–35.
- Dickinson AM, Wang XN, Sviland L, et al. In situ dissection of the graft-versus-host activities of cytotoxic T cells specific for minor histocompatibility antigens. *Nat Med*. 2002;8:410–4.

## CD137-guided isolation and expansion of antigen-specific CD8 cells for potential use in adoptive immunotherapy

Kazue Watanabe · Susumu Suzuki · Michi Kamei ·  
Shingo Toji · Takakazu Kawase · Toshitada Takahashi ·  
Kiyotaka Kuzushima · Yoshiki Akatsuka

Received: 20 September 2007 / Revised: 7 May 2008 / Accepted: 9 June 2008 / Published online: 5 August 2008  
© The Japanese Society of Hematology 2008

**Abstract** The efficient isolation and *ex vivo* expansion of antigen-specific T cells are crucial for successful adoptive immunotherapy against uncontrollable infections and cancers. Several methods have been reported for this purpose, for example, employing MHC-multimeric complexes, interferon-gamma secretion, and antibodies specific for molecules expressed on T-cell surfaces, including CD25, CD69, CD107a, CD137, and CD154. Of the latter, CD137 has been shown to be one of the most promising targets since

it is only expressed on CD8<sup>+</sup> T cells early after encountering antigen, while being almost undetectable on resting cells. However, detailed comparisons between CD137-based and other methods have not yet been conducted. In this study, we therefore compared three approaches (with CD137, CD107a, and tetramers) using HLA-A24-restricted CMV pp65 and EBV BRLF1 epitopes as model antigens. We found that the CD137-based isolation of antigen-stimulated CD8<sup>+</sup> T cells was comparable to tetramer-based sorting in terms of purity and superior to the other two methods in terms of subsequent cell expansion. The method was less applicable to CD4<sup>+</sup> T cells since their CD137 upregulation is not sufficiently high. Collectively, this approach is most likely to be optimal among the methods tested for the isolation and expansion of antigen-specific CD8<sup>+</sup> cells.

K.W. and S.T. are employees of Medical Biological Laboratories Co., Ltd. S.S. is a representative executive of T Cell Technologies, Inc. Y.A. has received financial support through collaboration with Medical Biological Laboratories Co., Ltd.

K. Watanabe (✉) · S. Toji  
Research Reagent Division, Medical Biological  
Laboratories Co., Ltd., 1063-103 Ohara,  
Terasawaoka, Ina, Nagano 396-0002, Japan  
e-mail: watanabe.kazue@mbl.co.jp

K. Watanabe · M. Kamei · T. Kawase · T. Takahashi ·  
K. Kuzushima · Y. Akatsuka (✉)  
Division of Immunology, Aichi Cancer Center Research  
Institute, 1-1 Kanokoden, Chikusa-ku, Nagoya,  
Aichi 464-8681, Japan  
e-mail: yakatsuk@aichi-cc.jp

S. Suzuki  
T Cell Technologies, Inc., 3-5-10 Marunouchi,  
Naka-ku, Nagoya 460-0002, Japan

M. Kamei  
Department of Pediatrics and Neonatology,  
Nagoya City University, Graduate School of Medical Science,  
Nagoya, Japan

K. Kuzushima  
Department of Cellular Oncology,  
Nagoya University Graduate School of Medicine, Nagoya, Japan

**Keywords** CD137 · Adoptive transfer ·  
Cytotoxic T lymphocyte · Sorting

### 1 Introduction

Patients under severe immunosuppression after organ transplantation or chemotherapy, or due to congenital/acquired immunodeficiency, are vulnerable to infections with viruses such as cytomegalovirus (CMV) and Epstein-Barr virus (EBV), which are major causes of morbidity and mortality. Although the advent of new antiviral drugs for CMV [1] or anti-CD20 antibodies for EBV-associated B cell malignancies [2] has improved the survival of patients at risk, the adoptive transfer of T cells specific for these viruses still remains an attractive strategy, especially when the viruses or virus-associated tumors are resistant to such agents [3]. The powerful antiviral effects of infused T cells have been reported in various clinical settings [4–6]. There

are two ways to compensate for immunodeficiency in patients: (1) the infusion of ex vivo-expanded viral antigen-specific T cells; and (2) direct transfusion of peripheral blood T cells from healthy donors when the patients receive allogeneic hematopoietic cell transplantation. Although the latter method is feasible, there is a risk of graft versus host disease and it usually takes at least a few weeks before antiviral T cells have effectively expanded in vivo [7]. In contrast, although the former method is cumbersome and also time-consuming one at the ex vivo step, it is expected to be more effective and safer since only armed and selected viral antigen-specific T cells are infused [8].

Recently, several methods to detect and positively sort T cells specific for antigens of interest have been reported. These include the sorting of T cells stained with peptide/MHC multimers, with antibodies that react to cell surface-exposed CD107 (LAMP1) [9, 10], cell surface-captured interferon-gamma (IFN- $\gamma$ ), with the aid of a special biphasic antibody [11], and CD137 [12] as a more antigen-specific activation marker than CD25 or CD69. Except in tetramer or multimer cases, T cells activated with whole antigen without prior knowledge of the restriction HLA alleles or epitopes have been shown to be positively selected by flow-sorting or with magnetic beads using any of the above-mentioned methods. As these methods are based on the specific functions of individual cells, it is not easy to determine which method is most feasible for routine immunological studies and clinical application. In this report, we compared the results using three methods (using tetramers, CD107a, and CD137), all of which require a single staining step, employing CMV pp65 and EBV BRLF1 epitopes as model antigens, focusing on their merits and limitations.

## 2 Materials and methods

### 2.1 Cells and culture media

Peripheral blood mononuclear cells (PBMCs) were isolated by centrifugation on a Ficoll density gradient. All blood samples were collected after obtaining written informed consent, and the study was approved by the institutional review board of Aichi Cancer Center. Primary T cell lines were induced in RPMI 1640 (Sigma-Aldrich, St. Louis, MO, USA) supplemented with 12.5 mM HEPES, 5% autologous plasma, penicillin/streptomycin, and 2 mM L-glutamine (referred to as T cell medium). Epstein-Barr virus-transformed B cells (B-LCL) were established by infecting an aliquot of PBMCs with B95-8 supernatant.

### 2.2 Antibodies, tetramers, and flow cytometric analysis

Antibodies used for sorting and phenotyping were as follows: anti-CD4-PC5, anti-CD8-PC5, anti-CD28-PE,

anti-CD45RA-PE, anti-CD45RO-FITC (all from Beckman Coulter Inc., Miami, FL, USA) anti-CD137-FITC (MBL, Nagoya, Japan), anti-CD107a-FITC (Southern Biotech, Birmingham, AL, USA), anti-CD137-PE (BD Biosciences, San Diego, CA, USA), and anti-CCR7-FITC (R&D systems, Minneapolis, MN, USA). For intracellular interferon (IFN)- $\gamma$  staining, anti-IFN- $\gamma$ -FITC was from MBL (Nagoya, Japan). HLA-A\*2402 CMVpp65, HLA-A\*0201 CMV pp65, HLA-A\*2402 EBV-BRLF1, and HLA-DRB1\*0101 EBNA1 tetramers were purchased from MBL (Nagoya, Japan). Cells were first stained with tetramers for 15 min at room temperature, and then stained with appropriate combinations of antibodies for 15 min on ice. Flow cytometric analysis of the cells was performed using a FACSCalibur (BD Biosciences) with the aid of CellQuest software (BD Biosciences).

### 2.3 Peptides

The following peptides were synthesized by BioSynthesis (Lewisville, TX, USA): CMV/pp65(341–349) (QYDP-VAALF, referred to as CMV-QYD hereafter), CMV/pp65(495–503) (NLVPMVATV, as CMV-NLV), EBV/BRLF1(320–328) (DYNFVKQLF, as EBV-DYN), and EBV/EBNA1(515–527) (TSLYNLRRGTALA, as EBV-TSL).

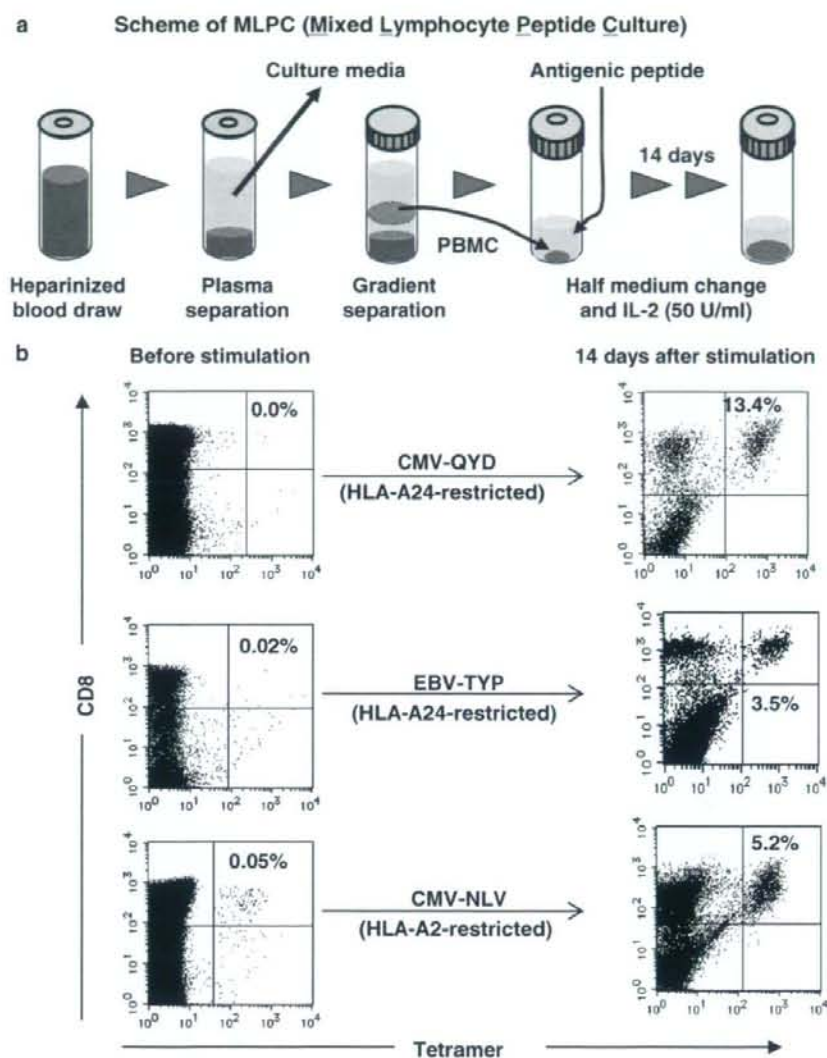
### 2.4 Induction of T cell lines by mixed lymphocyte-peptide cultures (MLPCs) (Fig. 1a)

The antigenic peptides listed above were directly added to PBMCs at 10  $\mu$ g/ml suspended in 2 ml T cell medium in a 15-ml round-bottomed tube (BD Biosciences), and the cultures were maintained at 37°C and 5% CO<sub>2</sub>. On day 2, recombinant human IL-2 (50 U/ml, Shionogi Pharmaceutical Institute Co., Osaka, Japan) was added. Starting on day 5, half-medium change and supplementation of IL-2 were performed every other day until day 14.

### 2.5 Restimulation and positive selection of antigen-specific T cells

Restimulation of MLPC T cell lines for the analysis of CD107a and CD137 expression followed by positive selection with MACS beads was performed 14 days after the primary stimulation. The optimal peptide concentration was predetermined for individual epitopes. Peptide was directly added to the aliquot of T cell lines without any antigen-presenting cells (APCs) and cytokines. For the determination of the optimal timing for positive selection either with anti-CD107a, or anti-CD137 antibody, the expression of CD107 and CD137 on antigen-specific T cells (identified by cognate tetramer) was assessed at

**Fig. 1** **a** Schematic diagram of mixed lymphocyte peptide culture (MLPC). Heparinized whole blood was first centrifuged to obtain plasma for culture media preparation. Peripheral blood mononuclear cells (PBMCs) were then separated by density gradient centrifugation from the resuspended blood pellets and cultured in RPMI1640 medium supplemented with 5% autologous plasma in the presence of 10  $\mu\text{g}/\text{ml}$  of antigenic peptide for 14 days. **b** Induction of viral antigen-specific T cell lines by MLPC. PBMCs were stained with the indicated tetramer before and after stimulation with the corresponding peptide. The percentages of tetramer<sup>+</sup> cells among CD3<sup>+</sup> populations are indicated. The data shown are representative of the following numbers of experiments: CMV-QYD,  $n = 17$ ; EBV-TYP,  $n = 10$ ; CMV-NLV,  $n = 5$



various time points. After incubation for the predetermined time, T cell lines were washed and stained with either FITC-labeled CD107a, or CD137 antibody at 10  $\mu\text{g}/\text{ml}$  in PBS containing 0.5% human serum albumin for 15 min at 4°C. After washing with MACS buffer (phosphate-buffered saline supplemented with 0.5% human serum albumin and 2 mM EDTA), the cells were incubated with anti-murine IgG1 MACS beads (Miltenyi Biotec, Auburn, CA, USA) for 15 min at 4°C. Cell separation was conducted using AutoMACS (Miltenyi Biotec). Antigen-specific T cells were also isolated without prior antigenic stimulation using cognate PE-conjugated tetramers followed by separation with anti-PE MACS beads and AutoMACS.

## 2.6 Expansion of sorted antigen-specific T cells

Sorted T cells were propagated in appropriately sized culture vessels in ALyS505N-1000 medium (Cell Science & Technology Institute, Inc., Sendai, Japan) originally containing 1000 U/ml of IL-2. Cultures were fed by changing half of the supernatant twice a week.

## 2.7 CFSE-based cytotoxicity assay

Target B-LCLs were labeled with 1  $\mu\text{M}$  6-carboxyfluorescein diacetate succinimidyl ester (CFSE; Wako Pure Chemical Industry, Osaka, Japan) for 10 min at 25°C.

After two washes, the CFSE-labeled target cells were cocultured with graded numbers of effector T cells for 5 h at 37°C and 5% CO<sub>2</sub> in the presence or absence of peptides in 96-well microtiter plates. The whole cells were harvested and stained with Annexin-V and Kusabira Orange (MBL) for 15 min at 25°C according to the manufacturer's instructions, and the absolute number of surviving cells was determined using a FACSCalibur with the aid of CellQuest software. The percentage lysis was calculated as follows:

$$\left[ \frac{(ET - T_0)}{(100 - T_0)} \right] \times 100.$$

ET indicates percentage of CFSE<sup>+</sup> Annexin-V<sup>+</sup> target cells cocultured with effector cells, and T<sub>0</sub> indicates the percentage of CFSE<sup>+</sup> Annexin-V<sup>+</sup> target cells without effector cells.

### 2.8 Statistical analysis

Data were expressed as the average ± SD of seven experiments. Samples were compared by paired Student's *t* test analyses using on-line software available at <http://www.physics.csbju.edu/stats/t-test.html>.

## 3 Results

### 3.1 Induction of viral antigen-specific T cell lines by MLPC

We first sought to determine whether a simple MLPC could expand cognate antigen-specific T cells from healthy donors serologically positive for CMV and/or EBV (Fig. 1a). As shown in Fig. 1b, 3–15% of CD8<sup>+</sup> tetramer<sup>+</sup> populations among surviving cells with the cultured PBMCs were readily obtained after 14 days of culture, although the magnitude of responses varied depending on the epitope peptides and donors. The induction of T cells from seronegative donors was not attempted.

### 3.2 Kinetics of CD107a and CD137 expression following stimulation

It is important to determine when the activation markers are maximally upregulated for optimal sorting. Although CD137 expression kinetics have been reported elsewhere [12], we made a comparison with those of CD107a. As shown in Fig. 2a, CD137 expression among tetramer<sup>+</sup> cells exceeded 90% around 16 h following stimulation with the predetermined minimal concentration (10 ng/ml, see below) of CMV-QYD peptide. The expression started to decline after 24 h, and only 25% of the cells remained positive after 48 h. In the case of CD107a, upregulation

was much quicker than with CD137, and a 70% level was maintained between 4 and 24 h, followed by a decline to 25% after 48 h. The maximal CD107a expression level was around 20% lower than that of CD137, and, unexpectedly, CD107a molecules exposed by the degranulation of CTLs remained on outer membranes for up to 24 h. Thus, we decided to perform the following positive selection experiments around 20 h after antigenic stimulation.

### 3.3 Optimization of peptide and primary antibody concentrations

Excessive antigenic stimulation is known to cause activation-induced cell death (AICD) in T cells [13]; thus, it is important to determine the minimal peptide concentration which results in sufficient CD137 expression. In the case of HLA-A24-restricted CMV-QYD peptide, the minimal concentration required to obtain more than 90% CD137<sup>+</sup> cells among the cognate tetramer<sup>+</sup> population was 10 ng/ml, and the use of 100 ng/ml resulted in a significant reduction of live cells, possibly due to AICD (Fig. 2b, c and data not shown). The optimal peptide concentrations differed among peptides; for example, 1 ng/ml was sufficient for the HLA-A24-restricted EBV-TYP peptide (data not shown), suggesting that the predetermination of optimal concentrations for individual peptides is necessary. A similar trend was observed when the extent of degranulation was assessed with CD107a antibody (data not shown).

The CD137 antibody (clone 4B4-1) itself does not induce AICD, but we also sought to determine sufficient concentrations by titration with measurement of the mean fluorescence intensity. In most cases, sufficient staining was obtained around 10 µg/ml (Fig. 2d and data not shown), which is a commonly employed concentration in most cell-staining procedures. Thus, we decided to use this concentration throughout the following experiments.

### 3.4 Comparison of three positive selection methods

Figure 3a shows the schematic procedures to positively select antigen-specific T cells by CD137, CD107a, or tetramer staining followed by MACS-based capture. In the case of tetramer-based sorting, peptide stimulation was not performed prior to sorting because it led to diminished tetramer staining, possibly due to the downregulation of T cell receptors (TCRs) on cognate T cells (upper right panel of Fig. 3b). The marked difference observed in sorted fractions just after positive selection was due to the fact that the tetramer-sorted fraction contained an average of 93% CD8<sup>+</sup> tetramer<sup>+</sup> cells (Table 1), while those obtained by CD107a and to lesser extent CD137 methods contained substantial numbers of tetramer<sup>-</sup> cells (Fig. 3b, second panel from the top). Since the tetramer<sup>-</sup> fractions were

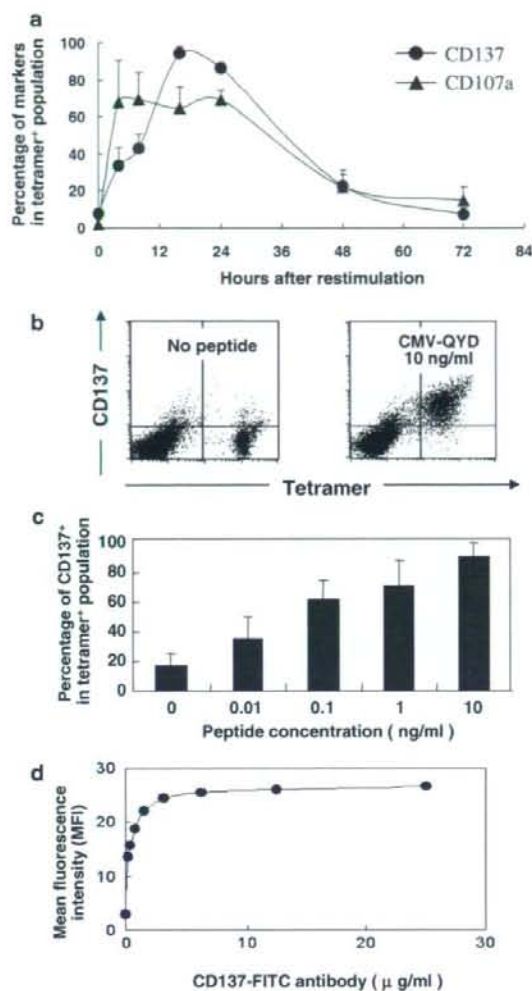


**Fig. 2** Optimization of conditions for positive selection. **a** Expression kinetics of CD137 and CD107a on T cells generated by MLPC with the CMV-QYD peptide. The percentages of indicated marker (CD137 or CD107a)-positive cells among tetramer<sup>+</sup> T cell populations after stimulation with 10 ng/ml CMV-QYD peptide are longitudinally plotted. The data shown are mean and SD values from four independent experiments. **b** A representative profile of CD137 expression before and after stimulation with the CMV-QYD peptide. **c** Titration of the CMV-QYD peptide for the full upregulation of CD137. T cell lines generated by MLPC with CMV-QYD peptide were restimulated with the indicated concentrations of peptide, and the percentages of CD137<sup>+</sup> cells among the tetramer<sup>+</sup> population were plotted. The data shown are mean and SD values from five independent experiments. **d** Titration of CD137 antibodies. The mean fluorescence intensity (MFI) of CD137 staining with graded concentrations of FITC-conjugated CD137 antibodies is shown. T cell lines were the same as used in **c** and were stimulated with 10 ng/ml CMV-QYD peptide for CD137 upregulation

composed of both CD8<sup>+</sup> and CD4<sup>+</sup> cells, it is likely that these fractions came from T cells that expressed CD137 or CD107a molecules nonspecifically. Antigen-independent, spontaneous CD137 upregulation in tetramer<sup>-</sup> cells was indeed present (Fig. 2b), which might explain the recovery of tetramer<sup>-</sup> cells by CD137- and CD107a-based sorting. However, following culture for 7 days, these tetramer<sup>-</sup> cells showed a trend toward disappearance, suggesting either the loss of the growth of cells that had been expressing CD137/CD107a non-relevant to antigen stimulation, or relative outgrowth of antigen-specific cells after sorting (Fig. 3b, bottom panels and Table 1).

Data regarding the recovery of CMV-QYD-specific T cells with the three sorting methods are summarized in Table 1. Due to a consistently high percentage (average >93%) of tetramer<sup>+</sup> cells in the tetramer-sorted fraction, the total recovery of tetramer<sup>+</sup> cells was also constant (34–44.5%). In Experiment 3, however, the poor cell recovery, especially with CD107a-based sorting using the AutoMACS device, was most likely caused by unexpectedly low CD107a induction (11.3% among tetramer<sup>+</sup> cells). Nevertheless, in the other two experiments, both CD137- and CD107a-based methods resulted in a better recovery of tetramer<sup>+</sup> cells than the tetramer-based method.

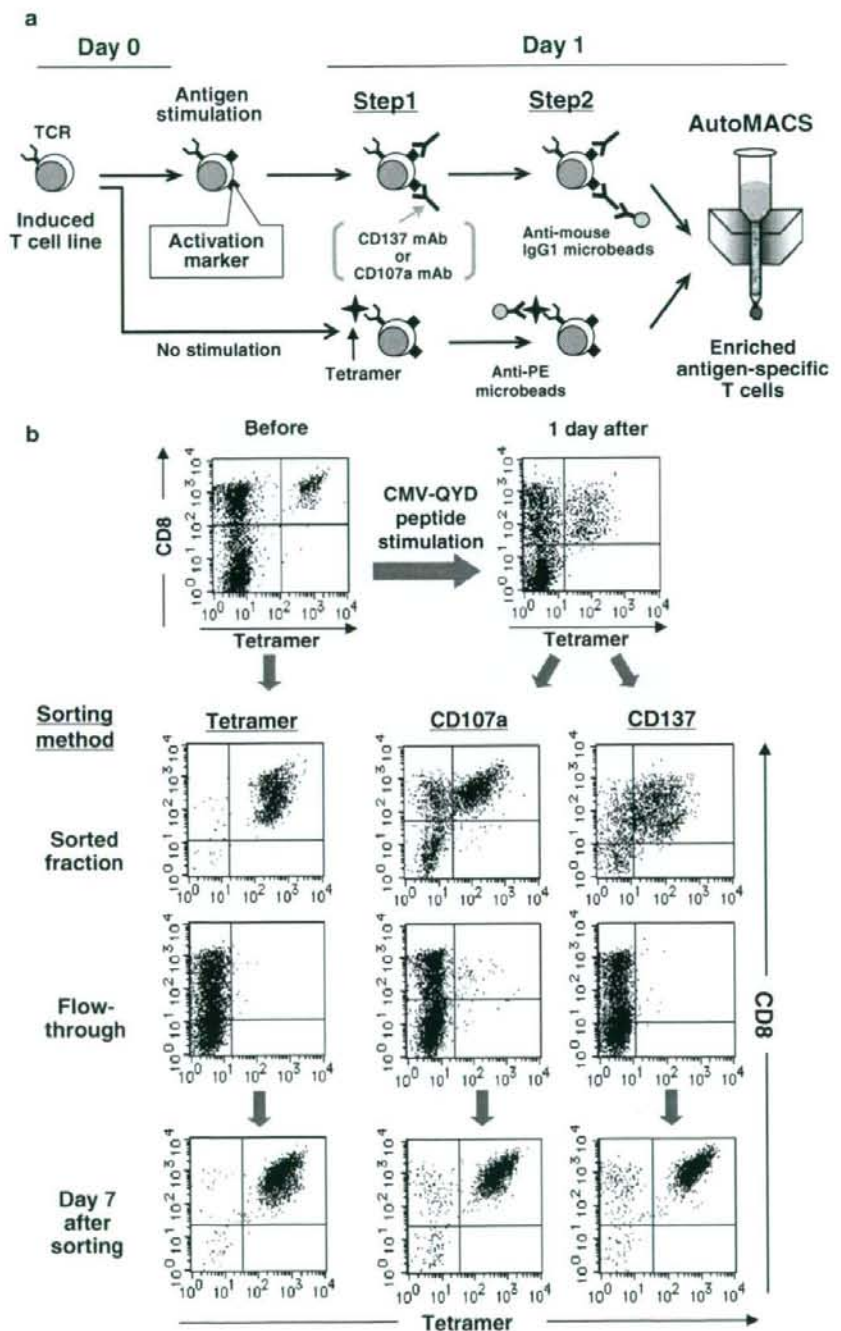
We next sought to determine which method was most suitable for expanding enriched antigen-specific T cells after sorting. Fig. 4a and b shows the growth kinetics of sorted fractions cultured in the presence of IL-2, but without any feeder cells for T cell lines specific for CMV-QYD (Fig. 4a) and EBV-TYP (Fig. 4b) obtained from seven individuals. In the CMV-QYD group, T cell lines enriched with the CD137-based method readily showed significantly better growth than those enriched with tetramer (Fig. 4a). In the EBV-TYP group, T cell lines enriched with the CD137-based method showed a trend toward better growth than those enriched with tetramer ( $P = 0.084$  for day 7 and  $P = 0.063$  for day 14, Fig. 4b). In the case of T cell lines enriched with CD107a, those specific for CMV-QYD showed moderate growth (Fig. 4a), while those specific for EBV-TYP remained unchanged in number (Fig. 4b). The difference of growth kinetics did not reach significance for CD137-based versus CD107a-based methods; however, there was a constant trend toward an increased number of antigen-specific T cells among the CD137-based sorting group (Fig. 4a, b).

### 3.5 Phenotype and functional aspects of T cell lines sorted by CD137

Since CD137-based enrichment gave promising results, especially with expansion after sorting, we further



**Fig. 3** Schematic illustration of positive selection using CD137, CD107a, or tetramer. **a** The MLPC-induced cell lines on days 14–16 after the initial stimulation were split and either restimulated with cognate antigenic peptide (2/3 part) or left without any stimulation (1/3 part) overnight. On the following day, T cells upregulating CD137 or CD107a by restimulation were first stained with individual antibodies and then incubated with anti-mouse IgG1 microbeads. T cells left untreated were first stained with cognate PE-conjugated tetramer and then incubated with anti-PE microbeads. T cells coated with the microbeads were then subjected to AutoMACS-based positive selection. **b** Representative flow cytometry data demonstrating the enrichment of CMV-QYD-specific T cells with the individual methods. The profiles of CD8<sup>+</sup> tetramer<sup>+</sup> cells in the AutoMACS-sorted, flow-through, and sorted fractions cultured for 7 days are shown



analyzed the phenotypes and functions of *in vitro*-expanded T cell lines obtained by the CD137 method. The CMV-QYD-specific T cell lines (gated by A24/

CMV-QYD tetramer staining) were mostly CD45RO<sup>+</sup> and CD45RA<sup>-</sup>, and more than a quarter of cells expressed both CCR7 and CD28, a hallmark for central memory

**Table 1** Comparison of the recoveries of CMV/QYD-specific T cells among the three sorting methods

	% tetramer <sup>+</sup> cells (day 0)	Method	% CD137 <sup>+</sup> or CD107a <sup>+</sup> among tetramer <sup>+</sup> cells	Number of tetramer <sup>+</sup> cells prior to sorting (day 1) ( $\times 10^5$ ) <sup>a</sup>	Sorted fraction (day 1)		
					% tetramer <sup>+</sup>	Number of tetramer <sup>+</sup> cells ( $\times 10^5$ )	% recovery of tetramer <sup>+</sup> cells
Experiment 1	8.3	CD137	95.6	6.4	66.3	3.7	58.0
		CD107a	95.0	6.4	58.4	3.3	51.1
		Tetramer	–	8.8	97.9	4.3	41.8
Experiment 2	12.4	CD137	98.3	1.74	80.8	1.29	74.1
		CD107a	87.3	1.74	75.2	0.98	56.3
		Tetramer	–	1.88	80.2	0.64	34.0
Experiment 3	22.5	CD137	99.2	23.8	96.0	2.88	12.1
		CD107a	11.3	23.8	32.1	0.29	1.2
		Tetramer	–	26.5	99.5	11.8	44.5

The experiment number corresponds to that shown in Fig. 4a

<sup>a</sup> Reduced number of tetramer<sup>+</sup> cells was caused mainly by activation-induced cell death during overnight stimulation with antigen

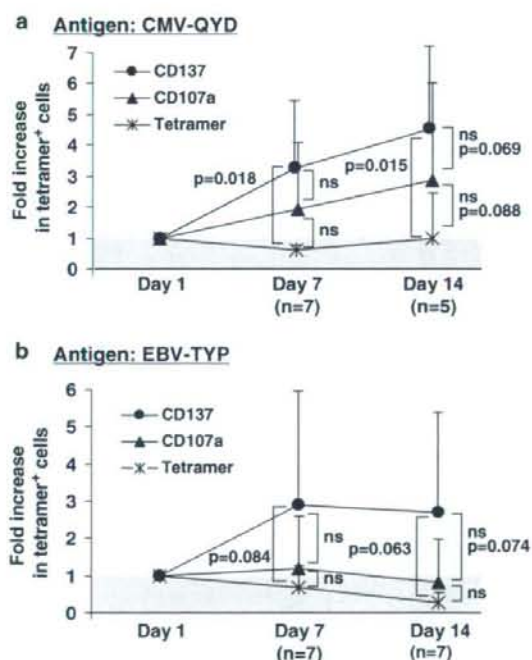


**Fig. 4** Expansion of enriched cells after sorting with CD137, CD107a, or tetramers. AutoMACS-sorted fractions were cultured in a 24- or 96-well culture plate in ALyS505N-1000 media containing 1,000 U/ml IL-2 for the indicated period. Average fold increases of cognate tetramer<sup>+</sup> cells from seven individuals including three shown in Table 1 are shown. **a** Expansion of CMV-QYD-specific T cell lines. **b** Expansion of EBV-TYP-specific T cell lines. Statistical values were obtained using paired Student's *t* test. The error bars represent the mean SD of the seven experiments except one including five experiments for CMV-QYD on day 14. *ns* not significant

T cells (Fig. 5a). Upon stimulation with cognate peptide (CMV-QYD), nearly half of the T cells could produce IFN- $\gamma$  (Fig. 5b). Finally, one of the T cell lines showed robust and specific lytic activity against CMV-QYD peptide-pulsed autologous B-LCLs (75% at an E/T ratio of 2, Fig. 5c).

### 3.6 Insufficient CD137 upregulation on antigen-stimulated CD4<sup>+</sup> T cells for positive selection

Since there is currently no feasible method to positively select antigen-specific CD4<sup>+</sup> cells, we examined whether CD137 might be sufficiently upregulated for MACS-based sorting. We first generated T cell lines by stimulating PBMC with an HLA-DRB1\*0101-restricted EBV-TSL peptide. Figure 6a shows a representative kinetic profile of CD137 expression on a T cell line before and after restimulation with EBV-TSL peptide. Percentages of CD137<sup>+</sup> cells among (CD4<sup>+</sup>) HLA-DRB1\*0101/EBV-TSL tetramer<sup>+</sup> cells increased from 8.4 to 40.4% after 16 h of stimulation, and declined to 14.6% at 48 h. However, the (CD4<sup>+</sup>) tetramer<sup>-</sup> fraction already showed upregulated CD137 expression before antigen stimulation, and its upregulation was more pronounced in terms of fluorescent intensity than that of the tetramer<sup>+</sup> fraction at 16 h, for unknown reasons (Fig. 6a, middle panel). As a result, although relatively more tetramer<sup>+</sup> CD137<sup>+</sup> cells were recovered in the sorted fraction (Fig. 6b, middle panels), the majority of tetramer<sup>+</sup> cells were eventually lost into the flow-through fraction, probably due to a weaker upregulation of CD137 insufficient for MACS-based sorting.

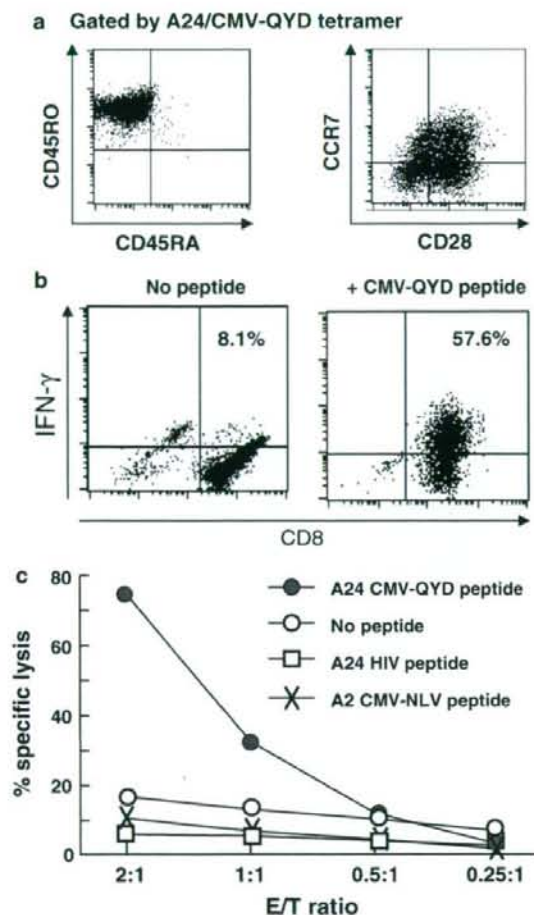


**Fig. 5** Phenotypes and functions of CD137-sorted and 7-day cultured T cell lines. **a** Representative flow cytometry profile of CMV-QYD-specific T cell lines for differentiation markers. T cells gated for the cognate tetramer were analyzed with the indicated markers. **b** Capacity for IFN- $\gamma$  production upon stimulation with autologous B-LCL pulsed with or without cognate peptide. **c** Cytotoxicity of T cell lines against peptide pulsed autologous B-LCL at the indicated effector:target (E:T) ratios. The data shown are representative of three independent experiments for **b** and **c**

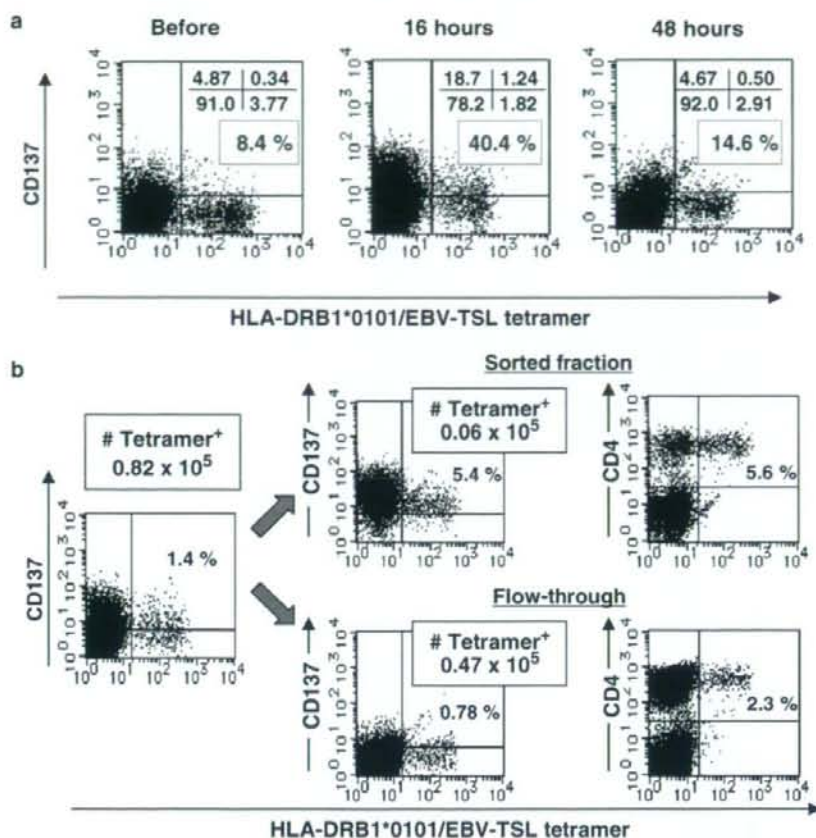
#### 4 Discussion

The enrichment of antigen-specific T cells is the first key step for successful adoptive immunotherapy, necessary to maximize efficacy and minimize unwanted reactivity to self-antigens that may result in autoimmunity. The present comparison of three methods (with CD137, CD107a, and HLA multimers) that can isolate T cells simply (i.e., by staining and separation with a MACS-based sorter) without any need for expensive flow cytometric cell sorters, showed a comparable recovery of antigen-specific CD8<sup>+</sup>

cells assessed by cognate tetramer staining. However, the CD137-based method was superior when cell proliferation following enrichment was also taken into consideration (Fig. 4), although the difference between this and the CD107a-based method did not reach significance, possibly due to limited number ( $n = 7$ ) of individuals tested and the inter-individual variation in the level of CD137 and CD107a upregulation after stimulation (data not shown). Nevertheless, the advantage of the CD137-based method is reasonable because CD137 has been shown to deliver a survival signal to activated T cells [14, 15]. In addition, CD137 was found to be upregulated in almost all (>90%) antigen-specific T cells, based on tetramer staining, when compared with CD107a (up to 70%), so that the former is likely to cover the full repertoire of antigen-specific T cells. Finally, we learned that CD137-based sorting is not suitable for antigen-specific CD4<sup>+</sup> T cells, at least with our current approach using simple “bulk” cultures, due to high background and bystander expression of CD137. However, CD137 was indeed upregulated upon antigen stimulation of cognate CD4<sup>+</sup> cells (Fig. 6a), as shown by others [16]. Because monocytes constitutively express CD137 (data not shown), the residual monocytes which were not killed by antigen-specific helper CD4<sup>+</sup> could contaminate the sorted fraction, likely resulting in the low-level purity of antigen-specific CD4<sup>+</sup> cells. To isolate antigen-specific CD4<sup>+</sup> helper T cells, the positive selection of CD154 or the CD40 ligand has been reported, although this method requires the addition of CD40-specific blocking antibodies to avoid the downregulation of CD154 induced by antigen stimulation [17]. We initially wished to isolate both antigen-specific CD8<sup>+</sup> and CD4<sup>+</sup> T cells with a single reagent, CD137, but our data demonstrated that it might be a suboptimal method at present, unless the IFN- $\gamma$  secretion assay, which requires two more steps, is performed [11].

In the current study, to induce cell surface CD137 or CD107a expression with antigenic peptides, they were simply added directly to PBMC suspensions without antigen-presenting cells in order to minimize in vitro manipulation. We stimulated PBMCs with a commonly used concentration (i.e., 10  $\mu\text{g}/\text{ml}$ ) of antigenic peptides for simplicity because resting memory T cells in PBMCs are relatively resistant to AICD compared to activated effector T cells [18]. Restimulation of in vitro-activated T cells just before positive selection, however, did induce moderate reduction of cognate T cells (data not shown), possibly due to AICD [18] or T cell versus T cell killing [19], whereby antigen-specific T cells presenting the pulsed peptide are killed by other antigen-specific T cells. AICD could be avoided using more precisely titrated concentrations of peptides, but this might be difficult since the occurrence of AICD may also depend on other factors, including the T cell activation status, co-existing cytokines, and

**Fig. 6** Induction of CD137 expression on antigen-specific CD4<sup>+</sup> T-cells. **a** PBMCs were stimulated in MLPC with the HLA-DRB1\*0101-restricted EBV-TSL peptide. On day 14 of culture, the T cells were stimulated with 10 ng/ml EBV-TSL peptide. The expression of CD137 was assessed along with HLA-DRB1\*0101/EBV-TSL tetramer staining before and 16 and 48 h after stimulation. **b** Representative flow cytometry data demonstrating the enrichment of EBV-TSL-specific T cells with the CD137-based method. The profiles of tetramer<sup>+</sup> cells counterstained with either CD137 (middle column) or CD4 (right column) in the AutoMACS-sorted and flow-through fractions are shown. Numbers in squares represent the absolute numbers of tetramer<sup>+</sup> cells, indicating the loss of most antigen-specific T cells into the flow-through fraction



costimulatory molecules [13]. The latter “mutual” killing could be avoided using peptide-pulsed autologous antigen-presenting cells; however, any usage of cells, even autologous, requires multiple steps, including thawing, washing, peptide pulsing, and irradiation, with which the risk of bacterial contamination may increase. Thus, the optimization of simple and safe restimulation conditions for the maximal induction of CD137 or CD107a while minimizing the loss of antigen-specific T cells should be further explored.

As previously shown, CD137- and CD107a-based methods can be performed without prior knowledge of precise peptide sequences or HLA restriction, unlike the tetramer-based approach. Although we used predetermined CMV- and EBV-derived peptides as model antigens in this study, we also confirmed that T cell enrichment followed by the cloning of minor histocompatibility antigen-specific T cells are possible with CD107a- or CD137-based sorting after T cell lines are restimulated using endogenously antigen-expressing PBMCs or B-LCLs (our unpublished

observations). This suggests that both methods are applicable for the positive selection of various T cell lines.

The long-term *in vitro* culture or expansion of T cells, especially after cloning, is known to be detrimental to T cell survival after returning to *in vivo* conditions due to progression to terminal differentiation [20]. Therefore, short-term induction culture, followed by enrichment and/or further short-term expansion are warranted. In our phenotypic and functional analyses, most T cells enriched with the CD137-based method and cultured for 7 days retained a central memory phenotype (Fig. 5a), IFN- $\gamma$  production capacity, and cytolytic activity when challenged with cognate antigen-presenting cells (Fig. 5b, c). Thus, short-term culture for 7 days did not result in the loss of critical functions of T cells necessary for adoptive immunotherapy. It has been shown that an average ninefold expansion over 8 days is possible for CD137-enriched cells when cultured in the presence of IL-2, IL-7 and, IL-15 [12]. In our expansion study, only an average 2.6-fold expansion was obtained. The difference might be caused partly

because we did not use IL-7 and IL-15, especially the latter, which is known to deliver anti-apoptotic signals and augment the proliferation and homeostasis of memory CD8<sup>+</sup> T-cells [21]. The other reason could be that we sorted antigen-specific cells from memory T cell pools of CMV- or EBV-seropositive individuals while others have employed CD45RA<sup>+</sup> naïve cells as a source of antigen-specific T cells [12]. Collectively, our data demonstrate that CD137-based sorting is indeed superior to other "one step" sorting methods.

**Acknowledgments** The authors thank Dr. Hiroki Torikai, Dr. Saitoko Morishima, Dr. Hidemasa Miyauchi, Dr. Ayako Demachi-Okamura, Ms. Yumi Nakao-Ohashi, Ms. Hiromi Tamaki, and Ms. Keiko Nishida for their expert technical assistance. This study was supported in part by Scientific Research on Priority Areas (B01) (no. 17016089), from the Ministry of Education, Culture, Science, Sports, and Technology, Japan; Research on Human Genome, Tissue Engineering Food Biotechnology and the Second and Third Team Comprehensive 10-year Strategy for Cancer Control (no. 26), from the Ministry of Health, Labour, and Collaboration with Medical Biological Laboratories Co., Ltd.

## References

1. Fishman JA, Emery V, Freeman R, et al. Cytomegalovirus in transplantation—challenging the status quo. *Clin Transplant*. 2007;21:149–58.
2. Ganne V, Siddiqi N, Kamalath B, et al. Humanized anti-CD20 monoclonal antibody (Rituximab) treatment for post-transplant lymphoproliferative disorder. *Clin Transplant*. 2003;17:417–22.
3. Gottschalk S, Heslop HE, Rooney CM. Adoptive immunotherapy for EBV-associated malignancies. *Leuk Lymphoma*. 2005;46:1–10.
4. Walter EA, Greenberg PD, Gilbert MJ, et al. Reconstitution of cellular immunity against cytomegalovirus in recipients of allogeneic bone marrow by transfer of T-cell clones from the donor. *N Engl J Med*. 1995;333:1038–44.
5. Heslop HE, Ng CY, Li C, et al. Long-term restoration of immunity against Epstein-Barr virus infection by adoptive transfer of gene-modified virus-specific T lymphocytes. *Nat Med*. 1996;2:551–5.
6. Savoldo B, Huls MH, Liu Z, et al. Autologous Epstein-Barr virus (EBV)-specific cytotoxic T cells for the treatment of persistent active EBV infection. *Blood*. 2002;100:4059–66.
7. Papadopoulos EB, Ladanyi M, Emanuel D, et al. Infusions of donor leukocytes to treat Epstein-Barr virus-associated lymphoproliferative disorders after allogeneic bone marrow transplantation. *N Engl J Med*. 1994;330:1185–91.
8. Riddell SR, Bleakley M, Nishida T, Berger C, Warren EH. Adoptive transfer of allogeneic antigen-specific T cells. *Biol Blood Marrow Transplant*. 2006;12:9–12.
9. Rubio V, Stuge TB, Singh N, et al. Ex vivo identification, isolation and analysis of tumor-cytolytic T cells. *Nat Med*. 2003;9:1377–82.
10. Betts MR, Brenchley JM, Price DA, et al. Sensitive and viable identification of antigen-specific CD8<sup>+</sup> T cells by a flow cytometric assay for degranulation. *J Immunol Methods*. 2003; 281:65–78.
11. Brosterhus H, Brings S, Leyendeckers H, et al. Enrichment and detection of live antigen-specific CD4(+) and CD8(+) T cells based on cytokine secretion. *Eur J Immunol*. 1999;29:4053–9.
12. Wolf M, Kuball J, Ho WY, et al. Activation-induced expression of CD137 permits detection, isolation, and expansion of the full repertoire of CD8<sup>+</sup> T cells responding to antigen without requiring knowledge of epitope specificities. *Blood*. 2007; 110:201–10.
13. Baumann S, Krueger A, Kirchhoff S, Krammer PH. Regulation of T cell apoptosis during the immune response. *Curr Mol Med*. 2002;2:257–72.
14. Watts TH. TNF/TNFR family members in costimulation of T cell responses. *Annu Rev Immunol*. 2005;23:23–68.
15. Wen T, Bukczynski J, Watts TH. 4-1BB ligand-mediated costimulation of human T cells induces CD4 and CD8 T cell expansion, cytokine production, and the development of cytolytic effector function. *J Immunol*. 2002;168:4897–906.
16. Wehler TC, Nonn M, Brandt B, et al. Targeting the activation-induced antigen CD137 can selectively deplete alloreactive T cells from antileukemic and antitumor donor T-cell lines. *Blood*. 2007;109:365–73.
17. Frensch M, Arbach O, Kirchhoff D, et al. Direct access to CD4<sup>+</sup> T cells specific for defined antigens according to CD154 expression. *Nat Med*. 2005;11:1118–24.
18. Sabbagh L, Kaech SM, Bourbonniere M, et al. The selective increase in caspase-3 expression in effector but not memory T cells allows susceptibility to apoptosis. *J Immunol*. 2004; 173:5425–33.
19. Burrows SR, Suhrbier A, Khanna R, Moss DJ. Rapid visual assay of cytotoxic T-cell specificity utilizing synthetic peptide induced T-cell–T-cell killing. *Immunology*. 1992;76:174–5.
20. Gattinoni L, Klebanoff CA, Palmer DC, et al. Acquisition of full effector function in vitro paradoxically impairs the in vivo antitumor efficacy of adoptively transferred CD8<sup>+</sup> T cells. *J Clin Invest*. 2005;115:1616–26.
21. Diab A, Cohen AD, Alpdogan O, Perales MA. IL-15: targeting CD8<sup>+</sup> T cells for immunotherapy. *Cytotherapy*. 2005;7:23–35.

## Identification of human minor histocompatibility antigens based on genetic association with highly parallel genotyping of pooled DNA

Takakazu Kawase,<sup>1,2</sup> Yasuhiro Nannya,<sup>3-5</sup> Hiroki Torikai,<sup>1</sup> Go Yamamoto,<sup>3-5</sup> Makoto Onizuka,<sup>6</sup> Satoko Morishima,<sup>1</sup> Kunio Tsujimura,<sup>7</sup> Koichi Miyamura,<sup>5,8</sup> Yoshihisa Koderu,<sup>5,8</sup> Yasuo Morishima,<sup>5,9</sup> Toshitada Takahashi,<sup>10</sup> Kiyotaka Kuzushima,<sup>1</sup> Seishi Ogawa,<sup>3-5</sup> and Yoshiki Akatsuka<sup>1,5</sup>

<sup>1</sup>Division of Immunology, <sup>2</sup>Division of Epidemiology and Prevention, Aichi Cancer Center Research Institute, Nagoya; <sup>3</sup>Department of Hematology/Oncology and <sup>4</sup>21st Century COE Program, Graduate School of Medicine, University of Tokyo, Tokyo; <sup>5</sup>Core Research for Evolutional Science and Technology, Japan Science and Technology Agency, Saitama; <sup>6</sup>Department of Genetic Information, Division of Molecular Life Science, Tokai University School of Medicine, Isehara; <sup>7</sup>Department of Microbiology and Immunology, Hamamatsu University School of Medicine, Hamamatsu; <sup>8</sup>Department of Hematology, Japanese Red Cross Nagoya First Hospital, Nagoya; <sup>9</sup>Department of Hematology and Cell Therapy, Aichi Cancer Center Hospital, Nagoya; and <sup>10</sup>Aichi Comprehensive Health Science Center, Aichi Health Promotion Foundation, Chita-gun, Japan

Minor histocompatibility (H) antigens are the molecular targets of allo-immunity responsible both for the development of antitumor effects and for graft-versus-host disease (GVHD) in allogeneic hematopoietic stem cell transplantation (allo-HSCT). However, despite their potential clinical use, our knowledge of human minor H antigens is largely limited by the lack of efficient methods of their characterization. Here we report a robust and efficient method of minor H gene discovery that combines whole genome associa-

tion scans (WGASs) with cytotoxic T-lymphocyte (CTL) assays, in which the genetic loci of minor H genes recognized by the CTL clones are precisely identified using pooled-DNA analysis of immortalized lymphoblastoid cell lines with/without susceptibility to those CTLs. Using this method, we have successfully mapped 2 loci: one previously characterized (*HMSD* encoding ACC-6), and one novel. The novel minor H antigen encoded by *BCL2A1* was identified within a 26 kb linkage disequilibrium block on

chromosome 15q25, which had been directly mapped by WGAS. The pool size required to identify these regions was no more than 100 individuals. Thus, once CTL clones are generated, this method should substantially facilitate discovery of minor H antigens applicable to targeted allo-immune therapies and also contribute to our understanding of human allo-immunity. (Blood. 2008;111:3286-3294)

© 2008 by The American Society of Hematology

### Introduction

Currently, allogeneic hematopoietic stem cell transplantation (allo-HSCT) has been established as one of the most effective therapeutic options for hematopoietic malignancies<sup>1</sup> and is also implicated as a promising approach for some solid cancers.<sup>2</sup> Its major therapeutic benefits are obtained from allo-immunity directed against patients' tumor cells (graft-versus-tumor [GVT] effects). However, the same kind of allo-immune reactions can also be directed against normal host tissues resulting in graft-versus-host disease (GVHD). In HLA-matched transplants, both GVT and GVHD are initiated by the recognition of HLA-bound polymorphic peptides, or minor histocompatibility (H) antigens, by donor T cells. Minor H antigens are typically encoded by dichotomous single nucleotide polymorphism (SNP) alleles, and may potentially be targeted by allo-immune reactions if the donor and recipient are mismatched at the minor H loci. Identification and characterization of minor H antigens that are specifically expressed in hematopoietic tissues, but not in other normal tissues, could contribute to the development of selective antileukemic therapies while minimizing unfavorable GVHD reactions, one of the most serious complications of allo-HSCT.<sup>3,4</sup> Unfortunately, the total number of such useful minor H antigens that are currently molecularly character-

ized is still disappointingly small, including HA-1,<sup>5</sup> HA-2,<sup>6</sup> ACC-1<sup>7</sup> and ACC-2,<sup>7</sup> DRN-7,<sup>8</sup> ACC-6,<sup>9</sup> LB-ADIR-1F,<sup>10</sup> HB-1,<sup>11</sup> LRH-1,<sup>12</sup> and 7A7-PANE1,<sup>13</sup> limiting the number of patients eligible for such GVT-oriented immunotherapy.

Several techniques have been developed to identify novel minor H antigens targeted by CTLs generated from patients who have undergone transplantation. Among these, linkage analysis based on the cytotoxicity of the CTL clones against panels of lymphoblastoid cell lines (B-LCLs) from large pedigrees was proposed as a novel genetic approach,<sup>14</sup> and has been successfully applied to identify novel minor H epitopes encoded by the *BCL2A1* and *P2RX5* genes.<sup>7,12</sup> Nevertheless, the technology is still largely limited by its resolution, especially when large segregating families are not available. Linkage analysis using B-LCL panels from the Centre d'Etude du Polymorphisme Humain (CEPH) could only localize minor H loci within a range of 1.64 Mb to 5.5 Mb, which still contained 11 to 46 genes.<sup>7,12,14</sup> thus requiring additional selection procedures to identify the actual minor H genes.

On the other hand, clinically relevant minor H antigens might be associated with common polymorphisms within the human

Submitted October 22, 2007; accepted December 19, 2007. Prepublished online as *Blood* First Edition paper, January 4, 2008; DOI 10.1182/blood-2007-10-118950.

T.K. and Y.N. contributed equally to this work.

The online version of this article contains a data supplement.

The publication costs of this article were defrayed in part by page charge payment. Therefore, and solely to indicate this fact, this article is hereby marked "advertisement" in accordance with 18 USC section 1734.

© 2008 by The American Society of Hematology

population, and therefore could be ideal targets of genetic association studies, considering recent advances of large-scale genotyping technologies and the assets of the International HapMap Project.<sup>15,16</sup> In this alternative genetic approach using the extensive linkage disequilibrium (LD) found within the human genome, target loci can be more efficiently localized within relatively small haplotype blocks without depending on limited numbers of recombination events, given the large number of genotyped genetic markers.<sup>17</sup> Moreover, since the presence of a target minor H allele in individual target cells can be determined by ordinary immunologic assays using minor H antigen-specific CTLs, the characterization of minor H antigens should be significantly more straightforward than identifying alleles associated with typical common complex diseases, for which typically weak-to-moderate genetic effects have been assumed.<sup>18</sup>

In this report, we describe a high-performance, cost-effective method for the identification of minor H antigens, in which whole genome association scans (WGASs) are performed based on SNP array analysis of pooled DNA samples constructed from cytotoxicity-positive (CTX<sup>+</sup>) and cytotoxicity-negative (CTX<sup>-</sup>) B-LCLs as determined by their susceptibility to CTL clones. Based on this method, termed WGA/CTL, we were able to map the previously characterized ACC-6 minor H locus to a 115-kb block containing only 4 genes, including *HMSD*.<sup>9</sup> Moreover, using the same approach, a novel minor H antigen encoded by the *BCL2A1* gene was identified within a 26-kb block containing only *BCL2A1* on chromosome 15q25. Surprisingly, the pool size required to identify these regions was no more than 100 individuals. Thus, this WGA/CTL method has significant potential to accelerate the discovery of minor H antigens that could be used in more selective, and thus more effective, allo-immune therapies in the near future.

## Methods

### Cell isolation and cell cultures

This study was approved by the institutional review board of the Aichi Cancer Center and the University of Tokyo. All blood or tissue samples were collected after written informed consent was obtained in accordance with the Declaration of Helsinki. B-LCLs were derived from allo-HSCT donors, recipients, and healthy volunteers. B-LCLs were maintained in RPMI 1640 medium supplemented with 10% fetal calf serum, 2 mM L-glutamine, 1 mM sodium pyruvate.

### Generation of CTL lines and clones

CTL lines were generated from peripheral blood mononuclear cells (PBMCs) obtained after transplantation by stimulation with irradiated (33 Gy) recipient PBMCs harvested before HSCT, thereafter stimulated weekly in RPMI 1640 supplemented with 10% pooled human serum and 2 mM L-glutamine. IL-2 was added on days 1 and 5 after the second and third stimulations. CTL clones were isolated by standard limiting dilution and expanded as previously described.<sup>7</sup> CTL-1B9 was isolated from PBMCs harvested on day 30 after transplantation from a patient receiving a marrow graft from his HLA-identical sibling (HLA A11, A24, B39, B51, Cw7, Cw14), and CTL-2A12 has been described recently.<sup>9</sup>

### Chromium release assay

Target cells were labeled with 0.1 mCi (3.7 MBq) of <sup>51</sup>Cr for 2 hours, and 10<sup>3</sup> target cells/well were mixed with CTL at the effector-to-target (E/T) ratio indicated in a standard 4-hour cytotoxicity. All assays were performed at least in duplicate. Percent specific lysis was calculated as follows: ((Experimental cpm - Spontaneous cpm) / (Maximum cpm - Spontaneous cpm)) × 100.

### Immunophenotyping by enzyme-linked immunosorbent assay

B-LCL cells (20 000 per well, which had been retrovirally transduced with restriction HLA cDNA for individual CTLs, if necessary) were plated in each well of 96-well round-bottomed plates, and corresponding CTL clones (10 000 per well) were added to each well. After overnight incubation at 37°C, 50 μL supernatant was collected and released IFN-γ was measured by standard enzyme-linked immunosorbent assay (ELISA).

### Construction of pooled DNA and microarray experiments

Genomic DNA was individually extracted from immunophenotyped B-LCLs. After DNA concentrations were measured and adjusted to 50 μg/mL using the PicoGreen dsDNA Quantitation Reagent (Molecular Probes, Eugene, OR), the DNA specimens from CTX<sup>+</sup> and CTX<sup>-</sup> B-LCLs were separately combined to generate individual pools. DNA pools were analyzed in pairs using Affymetrix GeneChip SNP-genotyping microarrays (Affymetrix, Tokyo, Japan) according to the manufacturer's protocol,<sup>19,20</sup> where 2 independent experiments were performed for each array type (for more detailed statistical analysis for generated microarray data, see Document S1, available on the *Blood* website; see the Supplemental Materials link at the top of the online article).

### Estimation of LD blocks

LD structures of the candidate loci were evaluated based on empirical data from the International Hap Map Project (<http://www.hapmap.org/>).<sup>15</sup> LD data for the relevant HapMap panels were downloaded from the HapMap web site and further analyzed using Haploview software (<http://www.broad.mit.edu/mpg/haploview/>).<sup>21</sup>

### Transfection of 293T cells and ELISA

Twenty thousand 293T cells retrovirally transduced with HLA-A\*2402 were plated in each well of 96-well flat-bottomed plates, cultured overnight at 37°C, then transfected with 0.12 μg of plasmid containing full-length *BCL2A1* cDNA generated from either the patient or his donor using Trans IT-293 (Mirus, Madison, WI). B-LCLs of the recipient and his donor were used as positive and negative controls, respectively. Ten thousand CTL-1B9 cells were added to each well 20 hours after transfection. After overnight incubation at 37°C, 50 μL of supernatant was collected and IFN-γ was measured by ELISA.

### SNP identification by direct sequencing

Complementary DNA prepared from B-LCLs was polymerase chain reaction (PCR) amplified for the coding region of *BCL2A1* using the following primers: sense: 5'-AG AAGATGACAGACTGTGAATTTGG-3'; antisense: 5'-TCAACAGTATTGCTTCAGGAGAG-3'.

PCR products were purified and directly sequenced with the same primer and BigDye Terminator kit (version 3.1) by using ABI PRISM 3100 (Applied Biosystems, Foster City, CA).

### Confirmatory SNP genotyping

Genotyping was carried out using fluorogenic 3'-minor groove binding (MGB) probes in a PCR assay. PCR was conducted in 10-μL reactions containing both allelic probes, 500 nM each of the primers, 1 × TaqMan Universal PCR Master Mix (Applied Biosystems), and 1 μL (100 ng) DNA. PCR cycling conditions were as follows: predenature, 50°C for 2 minutes, 95°C for 10 minutes, followed by 35 cycles of 92°C for 15 seconds and 60°C for 1 minute in a GeneAmp PCR System 9700 (Applied Biosystems). The PCR products were analyzed on an ABI 7900HT with the aid of SDS 2.2 software (Applied Biosystems).

### Epitope reconstitution assay

The candidate *BCL2A1*-encoded minor H epitope and its allelic counterpart (DYLQYVLQI) peptides were synthesized by standard Fmoc chemistry. <sup>51</sup>Cr-labeled CTX<sup>-</sup> donor B-LCLs were incubated with graded concentrations of the peptides and then used as targets in standard cytotoxicity assays.

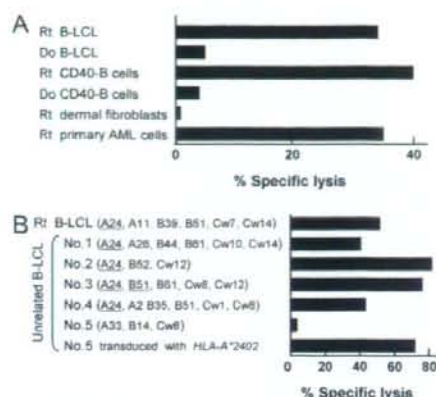


**Figure 1. Specificity of CTL-1B9 against hematopoietic cells and its restriction HLA.** (A) The cytotoxic activity of CTL-1B9 was evaluated in a standard 4-hour  $^{51}\text{Cr}$  release assay (E/T ratio, 20:1). Targets used were B-LCL, CD40-activated (CD40-B) B cells, dermal fibroblasts, and primary acute myeloid leukemia cells from the recipient (Rt), and B-LCL and CD40-B cells from his donor (Do). Rt dermal fibroblasts were pretreated with 500 U/mL IFN- $\gamma$  and 10 ng/mL TNF- $\alpha$  for 48 hours before  $^{51}\text{Cr}$  labeling. (B) Cytotoxic activity of CTL-1B9 against a panel of B-LCLs derived from unrelated individuals, each of whom shared 1 or 2 class I MHC allele(s) with the recipient from whom the CTL-1B9 was generated. The shared HLA allele(s) with the recipient are underlined. B-LCLs (no. 5) which did not share any HLA alleles with the recipient, were retrovirally transduced with HLA-A\*2402 cDNA and included to confirm HLA-A\*2402 restriction by CTL-1B9. Results are typical of 2 experiments and data are the mean plus or minus the standard deviation (SD) of triplicates.

## Results

### CTL-based typing and SNP array analysis of pooled DNA

CTL-2A12 and CTL-1B9 are CTL clones established from the peripheral blood of 2 patients with leukemia who had received HLA-identical sibling HSCTs. Each clone demonstrated specific lysis against the B-LCLs of the recipient but not against donor B-LCLs, indicating recognition of minor H antigen (Figure 1A and Kawase et al<sup>9</sup>). The minor H antigen for CTL-2A12 had been previously identified by expression cloning<sup>9</sup>; on the other hand, the target minor H antigen for the HLA-A24-restricted CTL-1B9 clone, which was apparently hematopoietic lineage-specific (Figure 1A) and present in approximately 80% of the Japanese population (data not shown), had not yet been determined. Using these CTL clones, a panel of B-LCLs expressing the restriction HLA (HLA-B44 for CTL-2A12 and HLA-A24 for CTL-1B9) endogenously or retrovirally transduced, were subjected to "immunophenotyping" for the presence or absence of the minor H antigen by ELISA and, if necessary, by standard chromium release assay (CRA). Based on the assay results, for CTL-2A12 we initially collected 44 cytotoxicity-positive (CTX<sup>+</sup>) and 44 cytotoxicity-negative (CTX<sup>-</sup>) B-LCLs after screening 132 B-LCLs, while 57 CTX<sup>+</sup> and 38 CTX<sup>-</sup> B-LCLs were obtained from 121 B-LCLs for CTL-1B9. From these sets of B-LCL panels, pools of DNA were generated and subjected to analysis on Affymetrix GeneChip 100 K and 500 K microarrays in duplicate.<sup>19,20</sup>

### Detection of association between minor H phenotypes and marker SNPs

Genetic mapping of the minor H locus was performed by identifying marker SNPs that showed statistically significant deviations in allele-frequencies between CTX<sup>+</sup> and CTX<sup>-</sup> pools based on the observed allele-specific signals in the microarray experiments. For



**Figure 2. Whole genome association scans performed with pooled DNA generated based on immunophenotyping with CTL-2A12.** Pooled DNAs generated from 44 CTX<sup>+</sup> and 44 CTX<sup>-</sup> B-LCLs were analyzed with 50 K XbaI (A), 50 K HindIII (B), 250 K NspI (C), and 250 K StyI (D) arrays. Test statistics were calculated for all SNPs and plotted in the chromosomal order. In all SNP array types, a common association peak is observed at 18q21, to which the minor H antigen for CTL-2A12, encoded by the *HMSD* gene, had been mapped based on expression cloning<sup>9</sup> (arrows).

this purpose, we evaluated the deviations of observed allele ratios between CTX<sup>+</sup> and CTX<sup>-</sup> pools for each SNP on a given array (Document S1). An SNP was considered as positive for association if its test statistic exceeded an empirically determined threshold that provided a "genome-wide" *P* value of .05 in duplicate experiments (Document S1, Figures S1,S2, and Table S1). Threshold values for different pool sizes are also provided in Table S2 for further experiments. The positive SNPs eventually obtained for both CTLs are summarized in Table 1, where the 10 SNPs showing the highest test statistics are listed for individual experiments.

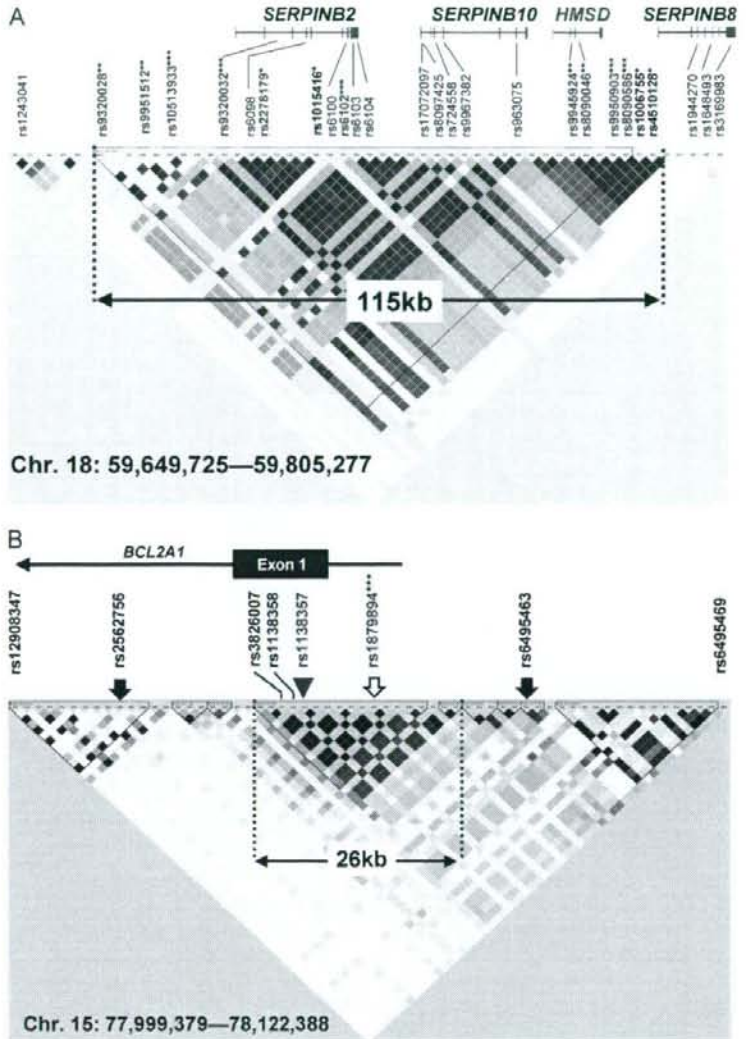
### Mapping of the minor H loci by WGASS

All the SNPs significantly associated with susceptibility to CTL-2A12 were correctly mapped within a single 115 kb LD block at chromosome 18q21 containing the *HMSD* gene (Figures 2 and 3A), which had been previously shown to encode the ACC-6 minor H antigen recognized by CTL-2A12.<sup>9</sup> According to the above criteria, no false-positive SNPs were reported in any array types (Table 1). Confirmation genotyping of individual B-LCLs from both panels revealed none of the 44 that had been immunophenotyped as CTX<sup>-</sup> were misjudged, while 8 of the 44 CTX<sup>+</sup> B-LCLs were found to actually carry no minor H-positive allele for ACC-6, which was likely due to the inclusion of individual B-LCLs showing borderline cytotoxicity (data not shown).

On the other hand, positive association of the target minor H antigen with CTL-1B9 was detected in 2 independent loci: SNP rs1879894 at 15q25.1 in 250 K *NspI* (Table 1, Figure 4A-B, and Figure S5) and SNP rs1842353 at 8q12.3 in 50 K *HindIII* (Table 1 and Figure S3A). We eventually focused on rs1879894, as it showed a much more significant genome-wide *P* value than SNP rs1842353 (Table 1). In contrast to the CTL-2A12 case, where many mutually correlated SNPs around the most significant one created a broad peak in the statistic plots (Figure 2 arrows and Figure S3), the adjacent SNPs (rs6495463 and rs2562756; Figure 3B solid arrows) around rs1879894 (Figure 3B open arrow) did not show large test statistic values, reflecting the fact that no marker SNPs on 100 K and 500 K arrays exist in high LD (Figure 3B dashed red lines encompassing 26 kb) with this SNP according to the HapMap data. To further confirm the association, we generated additional B-LCL pools consisting of 75 CTX<sup>+</sup> and 34 CTX<sup>-</sup>



**Figure 3. Linkage disequilibrium (LD) block mapped by CTL-2A12 and CTL-1B9.** (A) An LD block map identified by pairwise  $r^2$  plot from HapMap CEU data are overlaid with SNPs available from Affymetrix GeneChip SNP-genotyping microarrays (arrows) and 4 genes in the 115 kb block. SNPs that emerged repeatedly in the 2 independent experiments are indicated in blue. The genomewide  $P$  values for positive SNPs are shown as follows: \* $P < .05$ ; \*\* $P < .01$ ; \*\*\* $P < .001$ . The intronic SNP (rs9945924) controlling the alternative splicing of *HMSD* transcripts and expression of encoded ACC-6 minor H antigen is indicated in red. (B) LD blocks identified by pairwise  $r^2$  plot from HapMap JPT data are overlaid with SNPs available from Affymetrix GeneChip SNP-genotyping microarrays (arrows) and exon 1 of the *BCL2A1* gene. The only SNP showing a high association with CTL-1B9 immunophenotypes (rs1879894) is shown as an open arrow. The nonsynonymous SNP (rs1138357) controlling the expression of the minor H antigen recognized by CTL-1B9 is indicated by a red arrowhead. \*\*\*SNP with genomewide  $P < .001$ . The 2 SNPs adjacent to the 26 kb LD block (rs2562756 and rs6495463) never gave a significant genomewide  $P$  value.



B-LCLs from another set of 128 B-LCLs, and performed a WGAS. As expected, the WGAS of the second pools also identified the identical SNP with the highest test statistic value in duplicate experiments, unequivocally indicating that this SNP is truly associated with the minor H locus of interest (Figure 4C,D and Table S3). The association was also detected when the references in the first and second pools were swapped (data not shown).

#### Identification of the minor H epitope recognized by CTL-1B9

The LD block containing SNP rs1879894 that was singled out from more than 500 000 SNP markers with 2 sets of DNA pools only encodes exon 1 of *BCL2A1* (Figure 3B). To our surprise, this was the region to which we had previously mapped an HLA-A\*24-restricted minor H antigen, ACC-1.<sup>7</sup> We first confirmed that full-length *BCL2A1* cDNA cloned only from the recipient but not his donor could stimulate interferon- $\gamma$  secretion from CTL-1B9 when transduced into donor B-LCL (Figure 5A), indicating that *BCL2A1* is a bona fide gene encoding minor H antigen recognized

by CTL-1B9. We next genotyped 3 nonsynonymous SNPs in the *BCL2A1* exon 1 sequence (Figure 3B) and comparison was made between the genotypes and the susceptibility to CTL-1B9 of 9 HLA-A\*2402<sup>+</sup> B-LCLs, including ones generated from the recipient (from whom CTL-1B9 was established) and his donor. Susceptibility to CTL-1B9 correlated completely with the presence of guanine at SNP rs1138357 (nucleotide position 238, according to the mRNA sequence for NM\_004049.2) and thymine at SNP rs1138358 (nucleotide position 299) (Table 2), suggesting that the expression of the minor H epitope recognized by CTL-1B9 is controlled by either of these SNPs. We searched for nonameric amino acid sequences spanning the 2 SNPs using BIMAS software,<sup>22</sup> since most reported HLA-A\*2402 binding peptides contain 9 amino acid residues.<sup>23</sup> Among these, a nonameric peptide, DYLCQVLQI (the polymorphic residue being underlined), has a predicted binding score of 75 and was considered as a candidate minor H epitope. As shown in Figure 5B, the DYLCQVLQI was strongly recognized by CTL-1B9, whereas its allelic counterpart,

Table 1. Positive SNPs from pooled DNA analysis

CTL-2A12, Exp 1				CTL-2A12, Exp 2				CTL-1B9, Exp 1				CTL-1B9, Exp 2			
rsID	Chr	Position	$\Delta R_{A_{HLA}}$	rsID	Chr	Position	$\Delta R_{A_{HLA}}$	rsID	Chr	Position	$\Delta R_{A_{HLA}}$	rsID	Chr	Position	$\Delta R_{A_{HLA}}$
<b>50K X bal</b>															
<u>rs10513933</u>	18	59699669	0.366*	<u>rs10513933</u>	18	59699669	0.511†	rs1363258	5	103297593	0.239	rs10499174	6	131209689	0.352*
<u>rs9320028</u>	18	59668150	0.255†	<u>rs9320028</u>	18	59668150	0.360*	rs726083	3	67093729	0.203	rs30058	5	122325602	0.240
rs6102	18	59721450	0.221	rs10485873	7	3503743	0.157	rs639243	5	31392931	0.198	rs150724	16	61960443	0.213
rs724533	23	116440574	0.137	rs219323	14	59510440	0.150	rs1936461	10	56519024	0.186	rs1993129	8	63618836	0.208
rs1341112	6	104919391	0.136	rs10506892	12	82478539	0.147	rs763876	12	94922502	0.186	rs356946	13	69066751	0.201
rs470490	18	61182216	0.136	rs10492289	12	97786333	0.144	rs958404	7	133054441	0.179	rs2869268	4	86421898	0.184
rs2826718	21	21471423	0.134	rs10483466	14	35986827	0.139	rs10486727	7	41672315	0.178	rs287002	12	40312537	0.183
rs10506697	12	73241741	0.128	rs5910124	23	116408616	0.137	rs2833488	21	32010112	0.176	rs1146808	13	67688608	0.182
rs10506891	12	82393029	0.127	rs10512545	17	86337079	0.134	rs379212	5	60977687	0.172	rs10501287	11	42446011	0.180
rs308995	14	59657919	0.125	rs295678	5	58186928	0.131	rs1954004	14	58627872	0.170	rs564993	5	31393476	0.177
<b>50K HindIII</b>															
<u>rs9320032</u>	18	59712191	0.486†	<u>rs9320032</u>	18	59712191	0.506†	<u>rs1842353</u>	8	63617543	0.244*	rs9300692	13	101216476	0.225†
<u>rs8090046</u>	18	59773066	0.207†	<u>rs8090046</u>	18	59773066	0.245*	rs10521202	17	12755289	0.201†	<u>rs1842353</u>	8	63617543	0.210†
rs1474220	2	108525317	0.193†	rs10498752	6	41876488	0.210†	rs7899961	10	59696431	0.198†	rs10520983	5	31314700	0.195†
rs10498752	6	41876488	0.178	rs1941538	18	37994337	0.176	rs9320974	6	124421441	0.197†	rs1334373	13	80897038	0.173
rs2298578	21	21632551	0.167	rs7682170	4	152748018	0.174	rs10520983	5	31314700	0.179	rs10519164	15	75412758	0.163
rs7516032	1	91618962	0.165	rs1445862	5	3675257	0.169	rs1862446	5	147460749	0.170	rs9322063	6	146852196	0.152
rs5030938	10	70645922	0.164	rs4696976	4	21058616	0.167	rs1358778	20	13266796	0.169	rs8067384	17	37926265	0.150
rs1883041	21	44921845	0.158	rs5030938	10	70645922	0.165	rs1873790	4	83422480	0.166	rs10521202	17	12755289	0.147
rs3902916	4	189045176	0.155	rs3902916	4	189045176	0.165	rs1220724	4	70888705	0.162	rs7914904	10	62749969	0.141
rs1000551	20	58709208	0.154	rs1883041	21	44921845	0.164	rs9300692	13	101216476	0.157	rs1220724	4	70888705	0.141
<b>250K NspI</b>															
<u>rs9509003</u>	18	59781783	0.534†	<u>rs9509003</u>	18	59781783	1.036†	<u>rs1879894</u>	15	78055874	0.846†	<u>rs1879894</u>	15	78055874	1.072†
rs1463835	3	23539615	0.532†	<u>rs8090586</u>	18	59781864	0.518†	rs9646294	16	6110019	0.484†	rs6771859	3	190642054	0.387†
rs16975459	18	37802275	0.383†	rs6473170	8	80664840	0.338*	rs17734332	5	134945240	0.365†	rs10512261	9	98804394	0.299*
<u>rs8090586</u>	18	59781864	0.367*	rs4510128	18	59782312	0.310†	rs566619	7	41381538	0.345*	rs12122772	1	60384564	0.287*
rs16872621	4	22081055	0.312†	rs1006755	18	59782026	0.300†	rs17737566	6	50345280	0.310*	rs2153155	4	26034162	0.248†
rs870582	6	125097114	0.301†	rs7039378	9	118735938	0.258	rs3849955	9	28350374	0.285*	rs17126896	14	53320494	0.246†
rs1015416	18	59720363	0.270†	rs1860563	16	6418899	0.258	rs4616156	13	86581518	0.273*	rs1328652	13	35607527	0.240
rs2155907	11	97599883	0.227	rs4699126	4	105709109	0.212	rs2484698	1	217474460	0.263*	rs7021551	9	27446645	0.237
rs2112948	5	50994294	0.222	rs10275055	7	156212079	0.204	rs17139603	11	79638632	0.262*	rs252817	5	106752487	0.237
rs2919747	2	129681506	0.217	rs1526411	7	124658309	0.201	rs2156737	4	100642529	0.246†	rs10772587	12	12681356	0.235
<b>250K StyI</b>															
<u>rs6102</u>	18	59721450	0.597†	<u>rs6102</u>	18	59721450	0.495†	rs9383925	6	151975774	0.819†	rs201204	6	104842863	0.688†
<u>rs9951512</u>	18	59690885	0.374*	<u>rs9951512</u>	18	59771746	0.407*	rs6497397	16	19646258	0.311†	rs12556155	23	108836419	0.442†
rs6496897	15	90493249	0.320†	<u>rs9951512</u>	18	59690885	0.317†	rs917252	7	22219990	0.289†	rs4791422	17	10605304	0.435†
<u>rs9945924</u>	18	59771746	0.315†	rs1983205	3	157782892	0.314†	rs1019403	3	7823997	0.260†	rs7749012	6	106459559	0.336*
rs12707805	8	107404746	0.303†	rs950865	5	2720684	0.307†	rs17053134	5	155373544	0.259†	rs509951	5	31385483	0.308†
rs10971778	9	33893184	0.296†	<u>rs2278179</u>	18	59715512	0.292†	rs11710880	3	72214965	0.246	rs16879024	8	32225711	0.256†
rs6565076	16	81487818	0.294†	rs10427722	22	36417752	0.289†	rs17167866	7	13919264	0.237	rs21000054	15	75293482	0.252
<u>rs2278179</u>	18	59715512	0.291†	rs17156659	7	82046820	0.271	rs10867062	9	137935241	0.237	rs11811023	1	143805934	0.240
rs7806238	7	29906442	0.290†	rs4502324	18	4811261	0.262	rs5925800	23	23278707	0.235	rs17382798	15	75256074	0.231
rs965888	18	38062658	0.283†	rs1348428	2	225927288	0.260	rs2255831	4	146614313	0.234	rs2030302	17	12526591	0.231

Significant SNPs that appeared on both experiments are underlined.

\*Genomewide  $P < .01$ .†Genomewide  $P < .001$ .‡Genomewide  $P < .05$ .

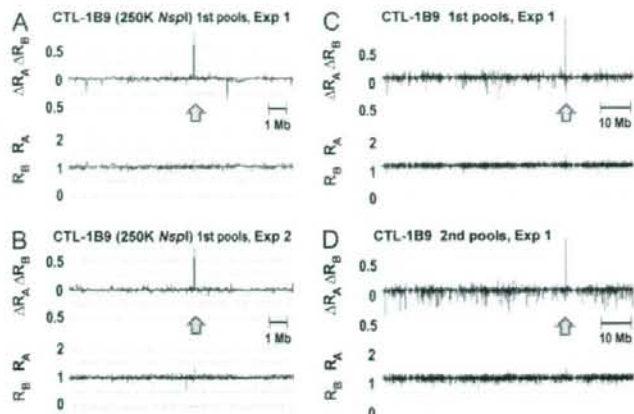
DYLQYVLQI, was not. Decameric peptide, QDYLCVQLQI, on the other hand, appeared to be weakly recognized; however, it is likely that the nonameric form was actually being presented after N-terminal glutamine cleavage by aminopeptidase in the culture medium. Because it was possible that the cystine might be cysteinylated, recognition of synthetic peptides DYLQCVLQI and cysteinylated DYLQCVLQI were assayed using CTL-1B9. Half-maximal lysis for the former was obtained at a concentration of 200 pM, whereas recognition of the latter was several-fold weaker (Figure 5C). Thus, we concluded that DYLQCVLQI defines the cognate HLA-A\*2402-restricted CTL-1B9 epitope, now designated ACC-1<sup>C</sup>. This incidentally provides a second example of products from both dichotomous SNP alleles being recognized as HLA-A\*2402-restricted minor H antigens, the first example being

the HB-1 minor H antigen.<sup>24</sup> Finally, real-time quantitative PCR revealed that T cells carrying the complementarity-determining region 3 sequence identical to CTL-1B9 became detectable in the patient's blood at the frequencies of 0.22%, 0.91%, 1.07% and 0.01% among TCR $\alpha\beta^+$  T cells at days 30, 102, 196, and 395 after transplantation, respectively, suggesting that ACC-1<sup>C</sup> minor H antigen is indeed immunogenic (Figure 5D).

## Discussion

Recent reports have unequivocally demonstrated that WGASs can be successfully used to identify common variants involved in a wide variety of human diseases.<sup>25-27</sup> Our report represents a novel

**Figure 4. Reproducible detection of association with the immunophenotypes determined by CTL-1B9 at the *BCL2A1* locus.** The maximum test statistic value was observed at a single SNP (rs1879894) within 15q25.1 in duplicate experiments for the first pools consisting of 57 CTX<sup>+</sup> and 38 CTX<sup>-</sup> B-LCLs (A-C). The peak association at the same SNP was reproduced in the experiments with the second pools consisting of 75 CTX<sup>+</sup> and 34 CTX<sup>-</sup> LCLs (D). Test statistic values ( $\Delta R_A \Delta R_B$ ) are plotted by blue lines together with their  $R_A$  (red) and  $R_B$  (green) values. The expected  $\Delta R_A \Delta R_B$  values multiplied by  $r^2$  correlation coefficients for the adjacent SNPs within 500 kb from the SNP rs1879894 are overlaid by red lines (A,B).



application of WGAs to transplantation immunology, which provides a simple but robust method to fine-map the genetic loci of minor H antigens whose expression is readily determined by standard immunophenotyping with CTL clones established from patients who have undergone transplantation.

The current WGA/CTL method has several desirable features that should contribute to the acceleration of minor H locus mapping. In comparing the method to those of linkage analysis and other nongenetic approaches, including direct peptide sequencing of chemically purified minor H antigens<sup>5,6,10,13</sup> and conventional

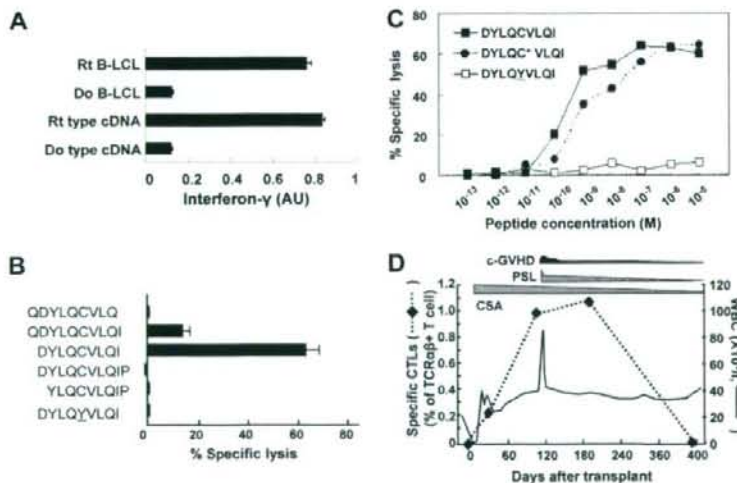


**Figure 5. Identification of the CTL-1B9 minimal minor H epitope.** (A) Interferon- $\gamma$  production from CTL-1B9 against HLA-A\*2402-transduced 293T cells transfected with plasmid encoding full-length *BCL2A1* cDNA cloned from either the recipient (Rt) from whom CTL-1B9 was isolated or his donor (Do). Rt B-LCL and Do B-LCL were used as positive and negative controls, respectively. Secreted interferon- $\gamma$  was measured by ELISA and is expressed in arbitrary units (AUs) corresponding to optical density at 630 nm. Results are typical of 2 experiments and data are the mean plus or minus SD of triplicates. (B) A peptide reconstitution assay was conducted to determine the minimal epitope for CTL-1B9. Nonameric peptide (DYLCQVLIQI), 2 nonameric peptides shifted by one amino acid to N- or C-terminus, N- and C-terminal extended decameric peptides, and its allelic counterpart (DYLYVLIQI) were synthesized and tested by adding to antigen-negative donor B-LCL at 10 nM in a standard <sup>51</sup>Cr release assay. Results are typical of 2 experiments and data are the mean plus or minus SD of triplicates. (C) Titration of the candidate minor H peptide by epitope reconstitution assay. Chromium-labeled donor B-LCLs were distributed to wells of 96-well round-bottomed plates, pulsed with serial dilutions of the indicated peptides for 30 minutes at room temperature, and then used as targets for CTL-1B9 in a standard <sup>51</sup>Cr release assay. A cysteinylated peptide (indicated by an asterisk) was included as an alternative form of the potential epitope. Results are typical of 2 experiments. (D) Tracking of ACC-1<sup>C</sup>-specific T cells in the recipient's peripheral blood. In order to longitudinally analyze the kinetics of the ACC-1<sup>C</sup>-specific CTLs in peripheral blood from the patient from whom CTL-1B9 was established, a real-time quantitative PCR was conducted. Complementary DNAs of peripheral blood mononuclear cells from the donor and patient before and after HSCT were prepared from the patient. Real-time PCR analysis was performed using a TaqMan assay as described previously.<sup>9</sup> The primers and fluorogenic probe sequences spanning the CTL-1B9 complementarity-determining region 3 (CDR3) were used to detect T cells carrying the CDR3 sequences identical to that of CTL-1B9. The primers and fluorogenic probe sequences spanning constant region of TCR beta chain (TCRBC) mRNA were used as internal control. Samples were quantified with the comparative CT method. The delta CT value was determined by subtracting the average CT value for TCRBC from the average CTL-1B9 CDR3 CT value. The standard curve for the proportion of CTL-1B9 among TCR $\beta^+$  T cells was composed by plotting mean delta CT values for each ratio, and the percentages of T cells carrying the CDR3 sequence identical to CTL-1B9 were calculated by using this standard curve. During this period, quiescent chronic GVHD, which required steroid treatment, developed; however, involvement of immune reaction to ACC-1<sup>C</sup> minor H antigen was unlikely since its frequency increased even after resolution of most chronic GVHD symptoms. c-GVHD, chronic GVHD; CSA, cyclosporine A; PSL, prednisolone; WBC, white blood cell count.

**Table 2. Correlation of BCL2A1 sequence polymorphisms with susceptibility to CTL-1B9**

	HLA-A*2402-positive B-LCLs								
	Rt	Do	UR1	UR2	UR3	UR4	UR5	UR6	UR7
Cytolysis by CTL-1B9	+	-	+	+	+	+	+	-	-
Detected SNP, position*									
rs1138357, 238	G/A	A	G	G	G/A	G/A	G/A	A	A
rs1138358, 299	T/G	G	T	T	T/G	T/G	T/G	G	G
rs3826007, 427	G	G/A	G	G	G	G	G/A	G/A	G

Rt indicates recipient; Do, donor; UR, unrelated; +, yes; and -, no.

\*Nucleotide positions are shown according to the NM\_004092.2 mRNA sequence, available at <http://www.ncbi.nlm.nih.gov/> as GEO accession GSE10044.

expression cloning,<sup>8,9,11</sup> there are differences in terms of power, sensitivity, and specificity. Direct sequencing of minor H antigen peptide guarantees that the purified peptide is surely present on the cell surface as antigen, but it requires highly specialized equipment and personnel. Expression screening of cDNA libraries is also widely used and has become feasible with commercially available systems. However, it depends highly on the quality of the cDNA library and expression levels of the target genes. In addition, it often suffers from false-positive results due to the forced expression of cDNA clones under a strong promoter. The current method of WGA/CTL genetically determines the relevant minor H antigen locus, not relying on highly technical protein chemistry using specialized equipment, or repetitive cell cloning procedures. It is also not affected by the expression levels of the target antigens.

As a genetic approach, the current method based on genetic association has several advantages over conventional linkage analysis: the mapping resolution has been greatly improved from several Mb in the conventional linkage analysis to the average haplotype block size of less than 100 kb,<sup>17,25-27</sup> usually containing a handful of candidate genes, compared with the dozens as typically found in linkage analysis. This means that the effort needed for the subsequent epitope mapping will be substantially reduced. In fact, the 115 kb region identified for CTL-2A12 contains 4 genes compared with 38 genes as revealed by the previous linkage study (data not shown), and the candidate gene was uniquely identified within the 26 kb region for CTL-1B9, for which linkage analysis had failed due to very rare segregating pedigrees among the CEPH panels with this trait (now ACC-1<sup>C</sup>; data not shown).<sup>15,16</sup> In addition, before moving on to epitope mapping, it would be possible to evaluate the clinical relevance of the minor H antigens by examining the tissue distribution of their expression, based on widely available gene expression databases such as Genomic Institute of the Novartis Research Foundation (GNF, <http://symatlas.gnf.org/SymAtlas/>).<sup>28</sup>

Second, the required sample size is generally small, and should be typically no more than 100 B-LCLs for common minor H alleles. This is in marked contrast to the association studies for common diseases, in which frequently thousands of samples are required.<sup>17,25-27</sup> In the current approach, sufficiently high test statistic values could be obtained for the relevant loci with a relatively small sample size, since the minor H allele is correctly segregated between the CTX<sup>+</sup> and CTX<sup>-</sup> pools by the highly specific immunologic assay. Combined with high accuracy in allelic measurements, this feature allows for the use of pooled DNAs in WGAS, which substantially saves cost and time, compared with the genotyping of individual samples. Unexpectedly, our method allows for a considerable degree of error in the immunophenotyping, indicating the robustness of the current method; in fact, the minor H locus for CTL-2A12 was successfully identified in spite of the presence of 8 (~10%) immunophenotyping errors. When the minor H allele has an extreme allele frequency

(eg, < 5% or > 95%), which could be predicted by preliminary immunophenotyping, WGAS/CTL may not be an efficient method of mapping, due to the impractically large numbers of B-LCLs that would need to be screened to obtain enough CTX<sup>+</sup> or CTX<sup>-</sup> B-LCLs. However, such minor H antigens would likely have limited clinical impact or applicability.

Sensitivity of the microarray analysis seems to be very high when the target SNP has good proxy SNPs on the array, because we were able to correctly identify the single SNP correlated with the target of CTL-1B9 from more than 500 000 SNP markers. On the other hand, genome coverage of the microarray is definitely important. In our experiments on CTL-2A12, the association was successfully identified by the marker SNPs showing  $r^2$  values of approximately 0.74 with the target locus of ACC-6. Since the GeneChip 500 K array set captures approximately 65% of all the HapMap phase II SNPs with more than 0.74 of  $r^2$ <sup>29</sup> and higher coverage will be obtained with the SNP 6.0 arrays having more than 1 000 K SNP markers, these arrays can be satisfactorily used as platforms for the WGA/CTL method.

As shown in the current study, the intrinsic sensitivity and specificity of the WGA/CTL method in detecting associated SNPs were excellent. In other words, as long as target SNPs are captured in high  $r^2$  values with one or more marker SNPs within the Affymetrix 500 K SNP set, there is a high likelihood of capturing the SNP with the current approach. To evaluate the probability of a given minor H antigen being captured in high  $r^2$  with marker SNPs, we checked the maximum  $r^2$  values of known minor H antigen SNPs with the Affymetrix 500 K SNPs, according to empirical data from the HapMap project ([www.hapmap.org](http://www.hapmap.org)). Among 13 known minor H antigens, 7 have their entries (designated minor H SNP) in the HapMap phase II SNP set (HA-3,<sup>30</sup> HA-8,<sup>31</sup> HB-1,<sup>11</sup> ACC-1 and ACC-2,<sup>7</sup> LB-ADIR-1F,<sup>10</sup> and 7A7-PANE1<sup>13</sup>), and were used for this purpose (note that absence of their entries in the HapMap data set does not necessarily mean that they could not be captured by a particular marker SNP set). As shown in Table S4, all 7 minor H SNPs are captured by at least one flanking SNP that is included in the Affymetrix 500 K SNP set with  $r^2$  values of more than 0.74 in at least one HapMap panel. The situation should be more favorable in the recently available SNP 6.0 array set with 1 000 K SNPs, indicating the genome coverage with currently available SNP arrays would be sufficient to capture typical minor H antigens with our approach.

Most patients who have received allo-HSCT could be a source of minor H antigen-specific CTL clones to be used for this assay, since the donor T cells are *in vivo* primed and many CTL clones could be established using currently available methods. In fact, substantial numbers of CTL clones have been established worldwide and could serve as the probes to identify novel minor H antigens.<sup>32,33</sup> Once constructed, a panel of B-LCLs, including those transduced with HLA cDNAs, could be commonly applied to immunophenotyping with different CTL clones, especially when